Technical Report *July 1971*

FEASIBILITY STUDY OF SLANTING FOR COMBINED NUCLEAR WEAPONS EFFECTS (Revised)

Volume 2: Appendices

Security F. Roon Filling From AirBlast

For:

OFFICE OF CIVIL DEFENSE
OFFICE OF THE SECRETARY OF THE ARMY
WASHINGTON, D.C. 20310

CONTRACT DAHC 20-67-C-0136
OCD Work Unit 1154E

SRI Project MU-6300-501

Approved for public release; distribution unlimited.

STANFORD RESEARCH INSTITUTE
Menlo Park, California 94025 · U.S.A.

PREFACE

This appendix is intended to serve both as a source of immediately applicable methodology and as a guide to the underlying gas dynamic theory. Those interested more in applying the methodology than in derivations and comparisons of calculated and observed results will find the following parts of this appendix of particular importance:

Location	Description
Section IIA	The simplest and fastest method of estimating average pressure in a room as a function of time; adequate for many purposes.
Section IIB3	Two different methods for a step-by-step, hand calculation providing average room pressure as well as dynamic pressure in the opening, valid for all flows through a single opening into a single room when the outside pressure is known as a function of time. Either method may be used but Method F is simpler for inflow, Method D for outflow; they may be combined in use.
Section IIC	Formulas for geometrical extent of the jet created inside the room by inflowing air and for dynamic pressure distribution within it.
Table E-3	A computer program to calculate average pressure within a single room and dynamic pressure in as many as eight openings as functions of time when a single room has openings into several different pressure fields (e.g., a room with front, rear, and side windows struck by a blast on the front wall).
Section IVB	A step-by-step hand calculation of average room pressure and dynamic pressure in each opening during filling of a single room through one or two openings into separate pressure fields.

When using the methodologies noted above, the user may find the meanings of symbols under Notation at the end of this appendix. Subscripts not explained there refer to physical spaces, i.e., subscript 1 indicates quantity is measured outside the room; other odd-numbered subscripts refer to interior of rooms and even-numbered subscripts refer to connecting ducts or openings.

CONTENTS

FIGURES

TABLES

Appendix E

ROOM FILLING FROM AIR BLAST

By J. R. Rempel

I Introduction

When a blast wave strikes a building, even should the structure withstand the initial impact, the resulting inflow of air through windows and other openings can be critical in determining the safety of any people sheltered by the structure and in determining the response of the structure itself to the blast impact. Although the physical laws obeyed by moving gases are well known and the course of the inflow in filling the building can in principle be calculated completely, any such calculation is far too lengthy to be practical for most purposes; fortunately, simplifications can be introduced which greatly shorten the labor of estimating effects of the blast inside the building and which give results in good to fair agreement with experiments done with small models. In general, the effect of the inflow is to provide a stream of fast moving air in the shelter space which may (1) endanger shelterees by hurling them against large relatively fixed objects or by hurling objects against them, and (2) provide a back pressure on the inner surfaces of structure walls countering the blast pressures on their outer surfaces.

Several factors enter into the calculation: the pressure outside each wall with openings and the time each opening becomes available, the area occupied by each opening and the volume of each room, the number of connected rooms and the area of each connection, and the ambient pressure and temperature in the building before the blast strikes. Perhaps the first of these to consider is what proportion of the wall exposed to the blast is open. If this fraction is greater than one half, the shock front leading the blast wave will pass into the building only slightly weakened and subsequent inside pressure should be estimated from a knowledge of shock position and the laws of shock reflection. Methods appropriate to this case are only touched upon here. On the other hand, should the fraction be less than one tenth, clearly the filling is not a shock process and the methods treated here are quite pertinent. Unfortunately, in many applications the fraction of open area will lie between these two extremes and, in these cases after the room filling calculation has been completed according to the methods suggested here, some thought must be given independently to the influence of the entering shock front.

When the source of the blast wave is an explosion and the location of the building in relation to the point of explosion is known or postulated, "free field" pressure histories at the building site can be found in standard references,[1,2,15]* and from these histories well known methods[1,3] are available to derive approximate histories on the outside of the walls of the building. Briefly, these methods account for a short-lived peak of pressure created by the impact of the front upon the wall nearest the explosion, the relatively fast erosion of this high pressure to a level which is the sum of the free field pressure plus a drag pressure on the wall due to the high winds behind the blast front. This quasi-steady pressure then decays slowly to zero as the blast wave moves onward past the structure.

Ordinary window glass breaks rather quickly, i.e., within 8 ms (milliseconds) or less when struck by blast overpressure of 1 psi (pound per square inch) or more.[4] Doors may withstand outside pressure longer, or even altogether. The time an opening becomes available with respect to the first impact of the blast upon the building becomes, then, the breaking time plus the time required by the wave to travel from the wall nearest the explosion to the opening. If the opening is in the wall nearest the explosion, travel time is of course zero. Strictly, the decay of the blast wave overpressure which occurs during this time must be taken into account, but when the blast arises from a nuclear explosion of yield greater than a few kt (kilotons) this decay is slight and negligible; that is, a single "free field" pressure history for all openings may be assumed.

It should be emphasized that the methods given here are simplified and their use can lead only to estimates. They are intended to provide: (1) calculations applicable to hand computation by those untrained in gas dynamics and (2) approximate results useful until more careful calculations are made. Only in the case of the simplest structural configurations and the simplest pressure history shapes can limits of error be suggested for these results. Such cases will be the subject of the discussion immediately below.

II Classical Nuclear Blast Wave Incident upon a Single Room

A. Estimation of Inside Pressure History

The "classical" blast wave from nuclear explosions consists of a steep pressure front or rise followed by a long-lasting decay phase during which the pressure in the wave falls to zero. It is accompanied by high winds giving rise to dynamic pressure against objects in the stream. Striking a wall at normal or near normal incidence, it creates a high pressure

---

* References are listed at the end of this Appendix.

zone at the surface, which however is rapidly eroded as relief waves move across the wall face from the edges. As a first approximation in the calculation of room filling, this reflected phase can usually be neglected. Following the decay of the high reflected pressure, the quasi-steady pressure (free field plus dynamic) remains against the wall for hundreds of milliseconds to several seconds, depending on explosive yield. Generally filling is complete before this quasi-steady pressure has fallen more than a few percent; hence, as a first approximation the outside pressure may often be considered constant and, if only a single wall with opening is exposed to the blast, the time ΔT (in milliseconds) to complete filling may be computed as the ratio $\frac{V}{2A}$, where V is room volume in cubic feet and A is area of opening in square feet.† The average room pressure at any time t during the filling process is then simply the fraction of the quasi-steady outside pressure given by the ratio $\frac{t}{\Delta T}$. For the purposes of this calculation, areas of several openings in the same wall should be added together to form the quantity A.*

In case there are two or more walls with openings exposed to the blast and each such wall sustains a different outside pressure history (as will happen, for example, when the drag coefficient is different for two walls), the calculation is more complicated but first estimates of filling time and average inside pressure during filling may be found by adding interior pressures calculated as if each wall alone were exposed. As an example, consider a room of volume 30'x10'x10' = 3000 ft^3 in which the front wall has total openings of 36 ft^2 and side walls have total openings of 60 ft^2. The ratios $\frac{V}{2A}$ for the front and side walls are 41.7 and 25 ft, respectively. If the quasi-steady overpressure on the front wall is 10 psig (pounds per square inch - gauge) and on the side wall 8 psig and if further the side wall opening becomes available 10 ms after the first blast impact, then the average inside pressure will be approximately as shown in Figure E-1 by the heavy line OAFG. In other words the room will fill in approximately 24 ms. Lines OAC and DE represent filling rates through front and side walls, respectively; and ordinates of OAC and DE are added to form the line OAFG. Of course after the average inside pressure exceeds 8 psi there will be outflow through the side wall; to allow for this loss the line FG has been placed between the outside pressure at the side wall (8 psig) and the outside pressure at the front wall (10 psig). The ordinate at FG is closer to 8 psig than to 10 psig because the area of the opening in the side wall is greater than that in the front wall. The line FG is intended to represent the final quasi-equilibrium pressure in the room.

---

* The experimental justification of most of the procedures described in this section is demonstrated later in Figures E-4, E-5, E-6 and E-8.

† Empirical relationship, dimensionally inconsistent. Meanings of symbols as used in this Appendix are defined as introduced and under "Notation" at end of Appendix.

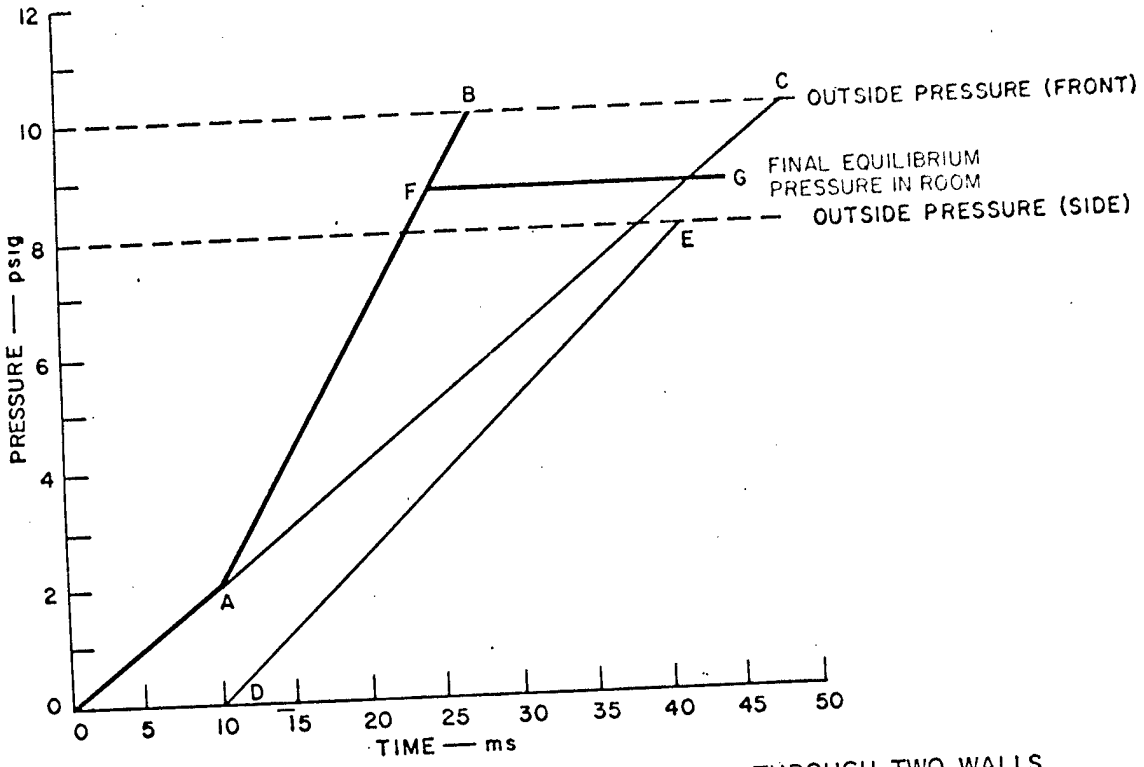

FIGURE E-1 APPROXIMATE FILLING RATES THROUGH TWO WALLS

These simple calculations do not apply when the reflected pressure lasts an appreciable length of time, or when the wave is non-classical such as it would be were a precursor present. Under these conditions the more detailed methods set forth below must be followed.

B. General Case

Justification for use of the simple methods noted above rests upon experience with a step-by-step calculation and comparison of its results with experiments. This calculation applies the principles of steady isentropic flow in ducts in successive, small time intervals. Conditions computed for the end of one time step become initial conditions for the next step. Conservation of energy, momentum and mass along with the assumption that the air behaves as a perfect gas with constant specific heats determine the thermodynamic variables, pressure, temperature and density, as well as the wind speed through the opening. Unique expressions lending themselves to simple calculation cannot be given for the laws of conservation of energy and momentum, and alternate forms leading to somewhat different results will be stated. All such expressions rely upon certain approximations to the conservation laws and these approximations usually introduce errors into the results in comparison with which the approximations arising in the assumptions of isentropy, perfect gas behavior and constant specific heats are negligible.

1. Inflow. Figure E-2 shows the idealized room with a single opening struck head-on by a blast wave. Three regions are noted: the outside ①, the doorway ② which serves as a duct connecting the outside with the room ③. In order to make the calculations tractable, uniformity of conditions in each of the two regions ① and ③ and over the cross section of region ② is assumed; furthermore, during each small time interval Δt, steady conditions are assumed in each region. During the aforementioned quasi-steady state outside the building these assumptions are probably valid for region ① but they clearly introduce error if the reflection or diffraction phase lasts an appreciable time, for during that episode relief waves are moving into the region from the edges of the building as well as from the doorway itself causing rapid fluctuations in wind speed and pressure. (Some account is taken of changes in pressure during the diffraction episode by the standard techniques of estimating outside pressure.) Similar remarks can be made concerning regions ② and ③, but if we are content to deal with "average" pressure and speed in those two regions, we may apply the step-by-step isentropic analysis. However, our present methods do not provide for any apportionment of gaseous energy in region ③ between streaming kinetic energy and internal energy; for simplicity of calculation it will be treated as entirely internal at all times, which will cause overestimation of pressure and neglect of winds within the chamber. In evaluating the wind threat, the speed and dynamic pressure in the duct ② must be regarded as the upper bounds on wind speed and dynamic pressure in region ③. Later, methods will be given for estimating change in dynamic pressure as the wind moves into the room.

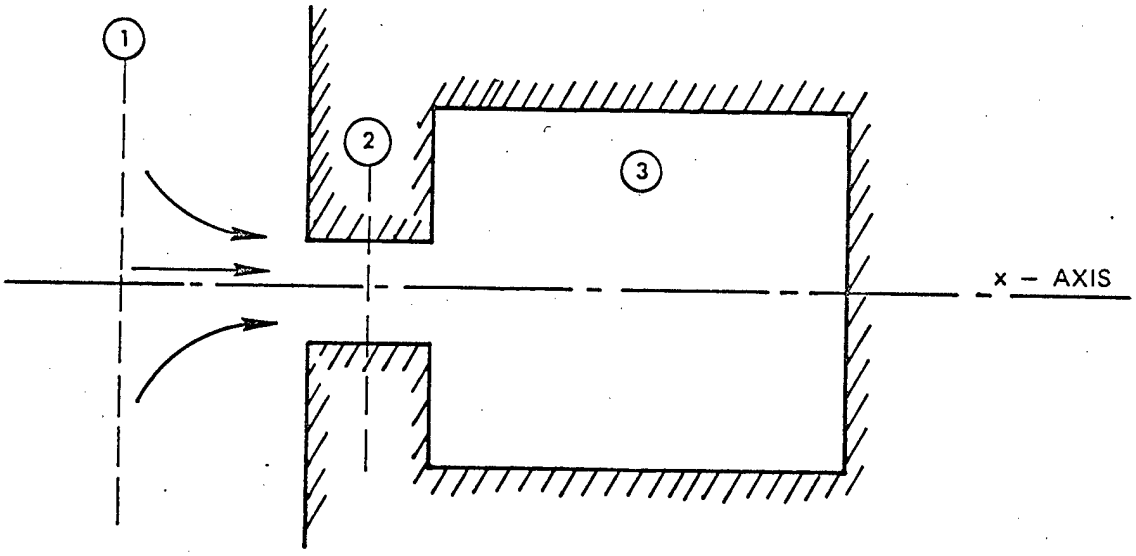

FIGURE E-2 THE FILLING CHAMBER

In writing the conservation equations, two views can be taken of conditions in region ①. On the one hand pressure, density and wind speed may be those of the free field behind the blast front or, on the other hand, the air upstream of the opening may be treated as stagnate at a pressure above free field either by the amount of the reflected pressure or by the amount of the product of the drag coefficient and dynamic pressure. Provided drag coefficients are known, the second view is more simply applied, especially when the blast front does not meet the wall head-on. In what follows, the pressure, P_1, and density, ρ_1, in region ① will be those of stagnate air outside the wall. The work done in moving a mass element Δm in region ① through a small distance Δx toward region ② is:

$$P_1 A_1 dx = P_1 \Delta V_1 = \frac{P_1}{\rho_1} \cdot \Delta m$$

where A_1 is the cross sectional area, and ΔV is the volume occupied by Δm in region ①. The mass element carries with it the internal energy it had in region ①, i.e.,

$$\frac{1}{\gamma - 1} \cdot \frac{P_1}{\rho_1} \cdot \Delta m,$$

where γ is the ratio of specific heat at constant pressure to the specific heat at constant volume. (The perfect gas equation of state is assumed; see Ref. 5.) If the flow into the room is steady, energy conservation requires that the same total energy, specifically, the sum

$$\frac{1}{\gamma - 1} \cdot \frac{P_1}{\rho_1} \cdot \Delta m + \frac{P_1}{\rho_1} \cdot \Delta m = \frac{\gamma}{\gamma - 1} \cdot \frac{P_1}{\rho_1} \cdot \Delta m$$

be given up within region ② during the same time interval. Furthermore mass conservation asserts that the mass element moving through region ② toward region ③ equal Δm. The work done in region ② in pressing the mass element toward region ③ is

$$\frac{P_2}{\rho_2} \cdot \Delta m$$

and the internal energy in the element is

$$\frac{1}{\gamma - 1} \cdot \frac{P_2}{\rho_2} \cdot \Delta m$$

where the subscript ② denotes conditions in region ②. Since the air is flowing into the room, however, the element in ② also carries (streaming) kinetic energy of amount

$$\frac{1}{2} u_2^2 \Delta m$$

where u designates particle or material speed. Thus, if conditions are not changing too fast, we can write (cancelling out the factor Δm):

$$\frac{\gamma}{\gamma - 1} \cdot \frac{P_1}{\rho_1} = \frac{\gamma}{\gamma - 1} \cdot \frac{P_2}{\rho_2} + \frac{1}{2} u_2^2 \qquad (1)$$

To apply conservation of linear momentum we consider a control surface, shown dashed in Figure E-3. Neglecting gravitational forces, the x-component of the force integrated over this surface must equal the rate of flow of the x-component of momentum out of the volume plus the rate of increase of x-momentum within the volume.[6] Neglecting frictional and viscous effects, the only force on the surface is the thermodynamic pres-

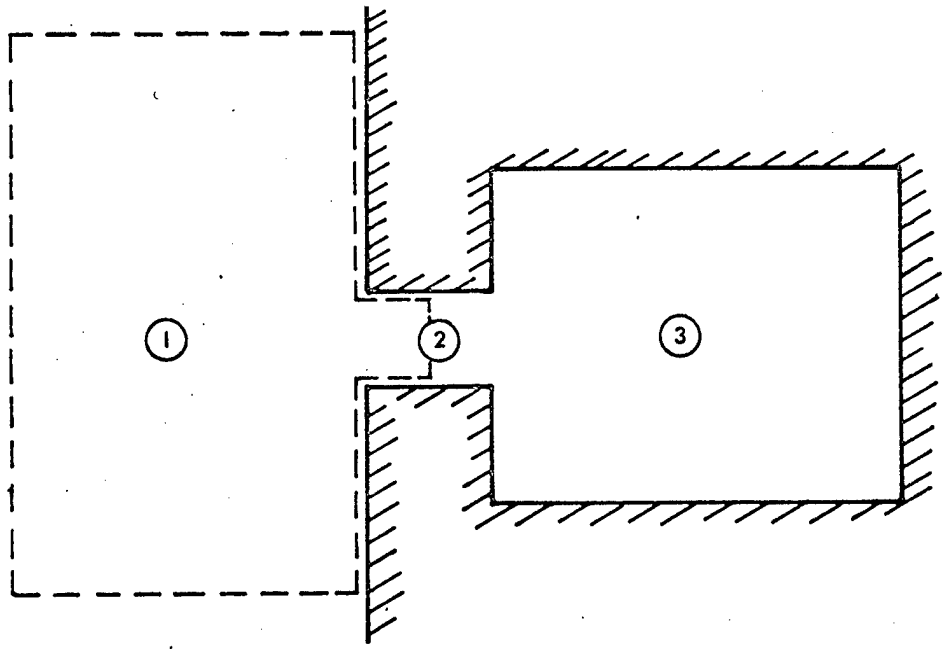

FIGURE E-3 FIRST CONTROL SURFACE

sure, exerted normal to the surface in an inward direction. Across the throat of the duct this pressure is taken to be P_2; everywhere else on the surface it is approximately P_1. (Around the entrance to the duct pressure on the wall will be less than P_1, but the mass flow rate turns out not to be highly sensitive to corrections made for this effect and, in order to simplify calculation, uniform pressure P_1 will be assumed. The mass speed u_2 however would be reduced by this correction.) During the quasi-steady episode momentum within the surface will change only slowly and we assume that it is in fact constant during each successive time increment Δt. (This assumption is clearly false during the shock diffraction episode due to the presence of fast moving reflected shock fronts within the surface. During the quasi-steady episode the assumption neglects the relief wave spreading into the stagnate air outside the opening.) Thus, carrying out the integration over the surface, we find

$$\int P \cos \theta \, da = (P_1 - P_2) A_2$$

In this integral θ is the angle between the inward normal to the surface and the positive x-direction and da is an element of area on the control surface. The total momentum in the positive x-direction passing through the surface is simply

$$\rho_2 u_2^2 A_2$$

Hence, momentum conservation reduces to

$$P_1 - P_2 = \rho_2 u_2^2 \tag{2}$$

Finally we note that even in the presence of moderately strong or weak shocks the isentropic equation of state of a perfect gas is accurate enough for this approximate calculation; hence

$$\rho_2 = \rho_1 \left[\frac{P_2}{P_1}\right]^{1/\gamma} \tag{3}$$

(See Ref. 7).

Given P_1 and ρ_1, Eqs. (1), (2), and (3) may be solved for P_2, ρ_2, and u_2.* The result can be written as:

---

* For diatomic gases like air, γ=1.4; see Ref. 8.

$$\frac{2\gamma}{\gamma + 1} \left[\frac{P_2}{P_1}\right]^{1/\gamma} = \frac{P_2}{P_1} + \frac{\gamma - 1}{\gamma + 1} \tag{4}$$

which is independent of ρ_1. If $y = \frac{P_2}{P_1}$, $A = \frac{\gamma - 1}{\gamma + 1}$

and $B = \frac{2\gamma}{\gamma + 1}$, Eq. (4) can be put in the form

$$By^{\frac{1}{\gamma}} = y + A \tag{5}$$

When A and B have the values stated above, Eq. (5) has two solutions, one of which is y = 1 and the other is y = 0.1912. The second solution is the only one of interest here and will be designated y_o.

To continue the calculation ρ_1 must be known. This value can be found from the Rankine-Hugoniot relations and knowledge of the strength and angle of incidence of the original shock front (Ref. 1,2), or it can, with enough accuracy for incident shock strengths less than 15 psi, be computed from ambient conditions using the isentropic equation of state, i.e.,

$$\rho_1 = \rho_o \left[\frac{P_1}{P_o}\right]^{1/\gamma} \tag{6}$$

where P_o and ρ_o are ambient pressure and density, respectively. With ρ_1 known, air density and pressure in the opening can be calculated from:

$$\rho_2 = \rho_1 \, y_o^{\,1/\gamma} \tag{7}$$

$$P_2 = y_o \, P_1 \tag{8}$$

from which wind speed becomes:

$$u_2 = \left[\frac{P_1 - P_2}{\rho_2}\right]^{\frac{1}{2}} = \left[\frac{P_1 \, (1 - y_o)}{\rho_1 \, y_o^{\,1/\gamma}}\right]^{\frac{1}{2}} \tag{9}$$

The mass flow into the room (3) can be written

$$\Delta m = \rho_2 \, u_2 \, A_2 \Delta t$$

$$= \left[P_1 \, (1 - y_o) \, y_o^{\frac{1}{\gamma}} \, \rho_1 \right]^{\frac{1}{2}} A_2 \, \Delta t \qquad (10)$$

If V_3 is the volume of the room and the prime is used to denote conditions in the room at the beginning of time step Δt, then average density in the room ρ_3 at the end of Δt can be written as:

$$\rho_3 = \rho_3' + \frac{\Delta m}{V_3} \qquad (11)$$

To find pressure in the room at the end of the time step we assume that all the energy lost in region (1) appears as an increase of internal energy of the gas in the room, i.e.,

$$\frac{\gamma}{\gamma - 1} \cdot \frac{P_1}{\rho_1} \cdot \Delta m = \frac{1}{\gamma - 1} \cdot \left(P_3 - P_3' \right) \; V_3$$

which can be solved to give P_3 in terms of known quantities:

$$P_3 = \frac{\gamma \, P_1}{\rho_1} \cdot \frac{\Delta m}{V_3} + P_3' \qquad (12)$$

At any time air temperature T_3 within the room can be calculated from the perfect gas law:

$$T_3 = \frac{P_3}{R \rho_3}$$

where R is the gas constant[5] for air in the appropriate units (e.g., in metric units R = 0.3028 joule/g^{o}C). The quantity T_3 can reach high values as a result of the compression existing behind the shock and within the room; however, if airflow to the outside (outflow) is maintained, the relaxation of pressure following the passage of the front will return room gas temperatures to safe levels before injury to occupants is likely. Only the long lasting increase in room temperature resulting from fires will normally be a threat to the shelterees.

Conditions existing in the chamber at the beginning of a time step are used in the foregoing calculations only in Eqs. (11) and (12) and do not influence duct parameters because transients have been omitted from consideration. Transient phenomena, for example, determine the direction of flow; that is, if $P_1 > P_3$, flow is inward as discussed above, but otherwise flow is outward. Repeated neglect of signals originating from the room leads to an accumulation of error in the calculation of average pressure as can be seen from comparisons between calculation as above and measurement shown in Figures E-4, E-5, and E-6. The experiments[9] were carried out in a 24-inch shock tube; the configuration of each model chamber is shown in an inset in the figure; and the foregoing calculation produces Curve F of the figures. The curves in Figures E-5 and E-6 labelled "external history (Λ)" are measurements in the free stream by means of a pitot tube oriented with respect to the stream to conform with the orientation of the opening in the model room; "external history" in Figure E-4 is side-on overpressure in the unobstructed shock tube.[9] In each case the calculation initially yields pressure in agreement with observation but eventually shows room pressure during filling in excess of measurement, although the maximum difference is 20% or less. Magnitude of Δt for these calculations was one-quarter the transit time of a sound signal across the room.

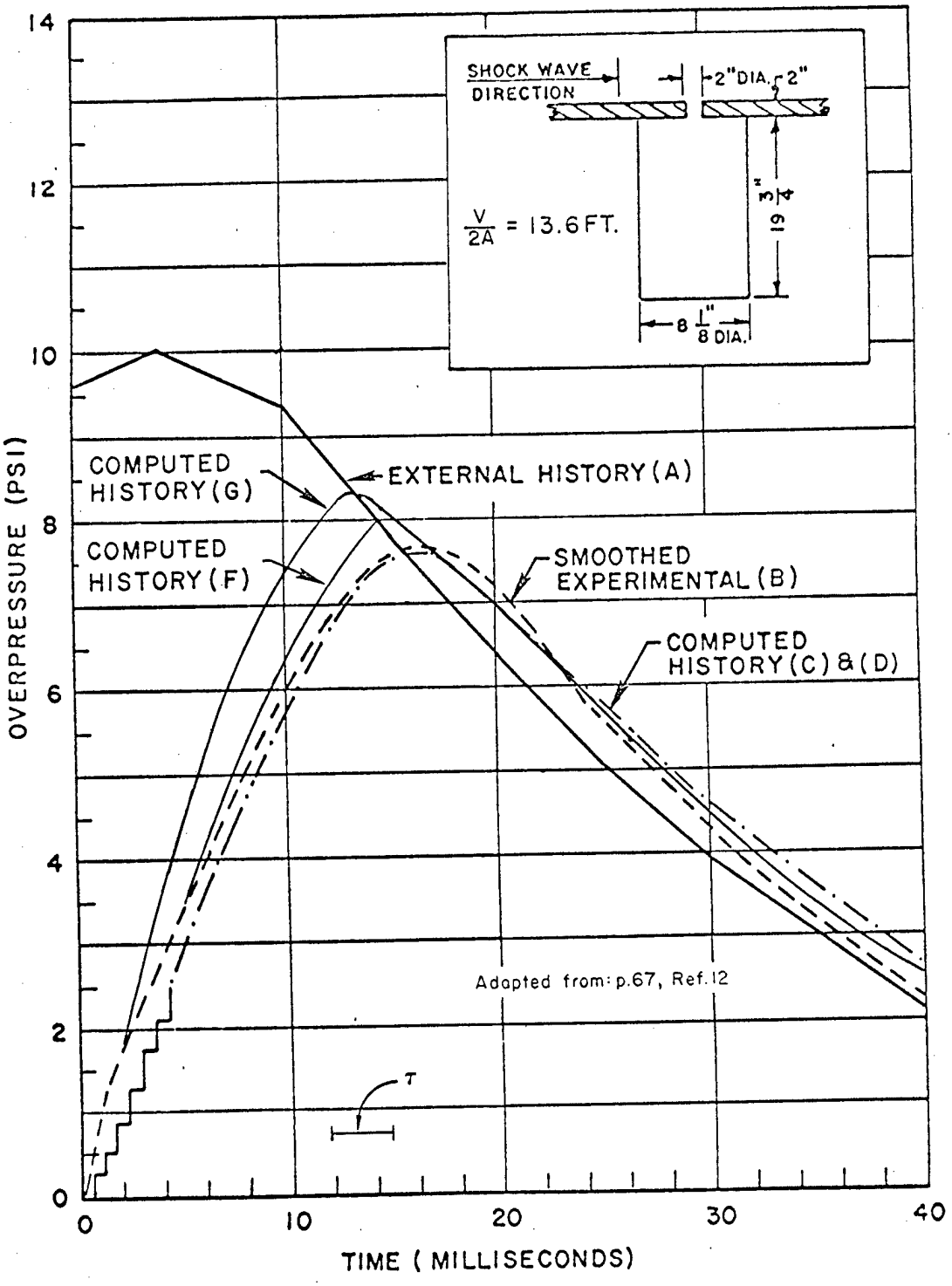

FIGURE E-4 FILL HISTORIES FOR SIDE-ON INCIDENCE

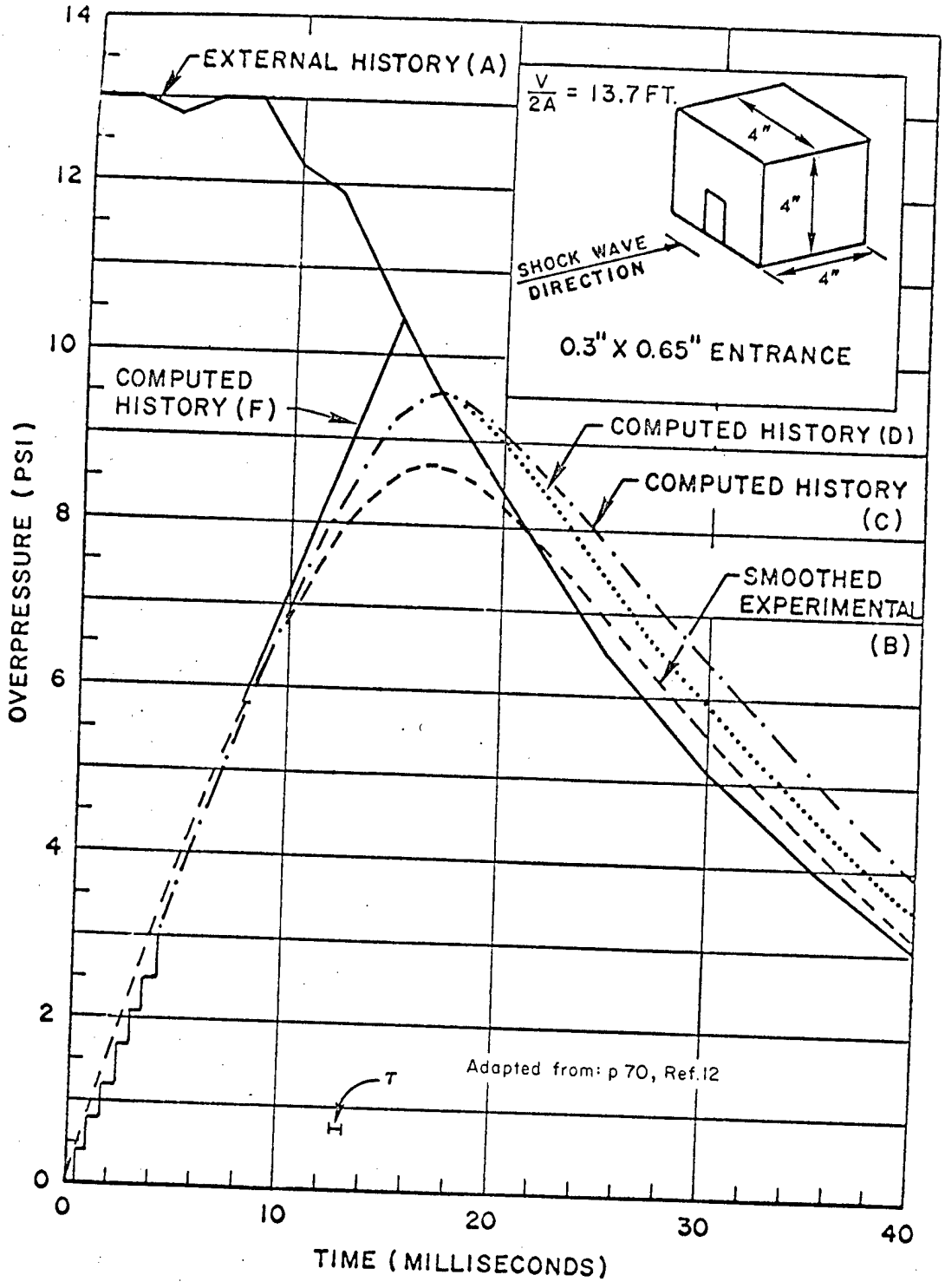

FIGURE E-5 FILL HISTORIES FOR A FACE-ON MODEL

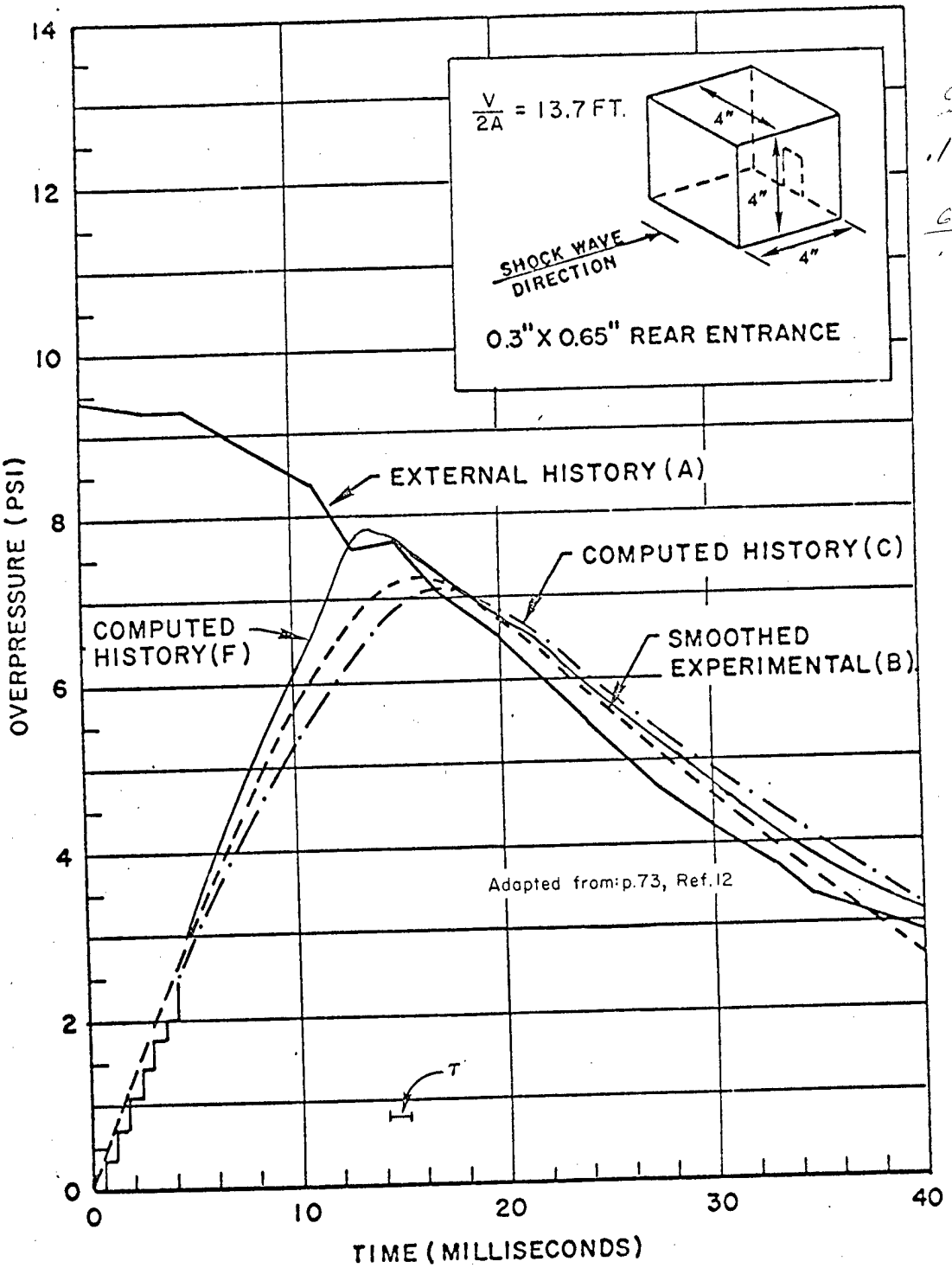

FIGURE E-6 FILL HISTORIES FOR A REAR FILL MODEL

Choice of the size of Δt is somewhat arbitrary except that (1) values much greater than sound transit time will give a false idea of the degree of irregularity in the fill process and (2) enough steps should be taken to make it possible for the influence of variations in P_1 to be shown in the results. The length of the bar labelled "τ" in Figures E-4, E-5, and E-6 represents the sound transit time across the longest room dimension.

The existence of significant theoretical errors in our treatment of flow into a room by quasi-steady analysis is clearly revealed by considering the single control surface formed by superposition of that shown in Figure E-3 and that indicated with dashed lines in Figure E-7. Such a surface coincides with the inner surfaces of the room and passage and extends into quiescent air outside. Under our hypotheses there is no flow through this surface anywhere and no change of momentum within it, yet the surface integral of the x-component of pressure over the boundaries does not vanish.

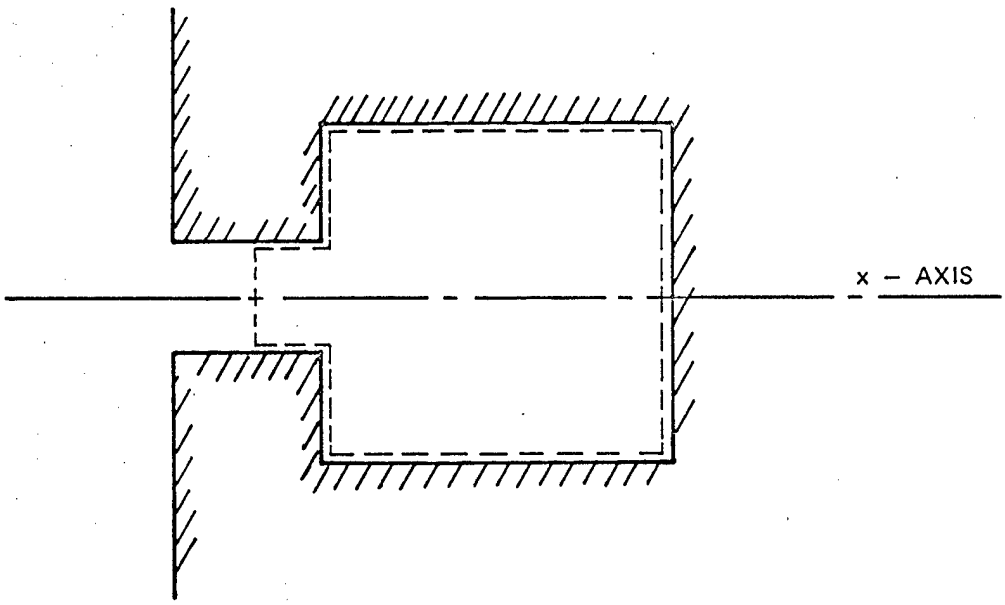

FIGURE E-7 SECOND CONTROL SURFACE

This absurdity can be avoided in one or both of two ways. A term may be added to the right side of Eq. (2) to account for the changing flow pattern within the control surface shown in Figure E-3 or a term may be added to the left side of Eq. (2) to account for the possible nonuniformity of pressure over the boundaries of the surface. As the room begins to fill, a rarefaction wave moves back into the high pressure gas outside the first doorway bringing more and more gas into motion toward the opening. In other words, the neglect of the rate of change with time of the momentum within the control surface outside the room may be at least one cause of the contradiction noted above. Any attempt to calculate a correction for this effect would certainly add to the complexity of these simplified procedures; furthermore, the degree of agreement between observations and theory of Method F (shown in Figures E-4, E-5, and E-6) suggests that the added effort to account for the rarefaction wave may not be needed to achieve the desired degree of accuracy.

Some writers[10,11,12,17] use the equation

$$P_2 = P_3' \tag{13}$$

instead of Eq. (2). Justification for Eq. (13) is based on analogy with the treatment of flow into a large chamber steadily being evacuated.[13] Equation (13) of course provides continual coupling between flow conditions and conditions in the room.

Using Eq. (13) we derive the pressure buildup inside the room in the following way. Substituting Eq. (3) into Eq. (1), then replacing P_2 with P_3' according to Eq. (13) and solving the resulting equation for u_2, we find:

$$u_2 = \left[\frac{2\gamma}{\gamma-1} \cdot \frac{P_1}{\rho_1} \left(1 - \left(\frac{P_3'}{P_1} \right)^{1-1/\gamma} \right) \right]^{1/2}$$

from which we calculate the mass inflow in the time increment Δt:

$$\begin{aligned} \Delta m &= K \rho_2 u_2 A_2 \Delta t \\ &= K \rho_1 \left(\frac{2\gamma}{\gamma-1} \cdot \frac{P_1}{\rho_1} \right)^{1/2} \left(\frac{P_3'}{P_1} \right)^{1/\gamma} \left[1 - \left(\frac{P_3'}{P_1} \right)^{1-1/\gamma} \right]^{1/2} A_2 \Delta t \end{aligned} \tag{14}$$

Whenever Eq. (13) is employed, empirical corrections must be made to reduce the calculated inflow rate or the calculation will not yield realistic values for room pressure in small experimental models; the simplest correction is the discharge coefficient,[13] represented by the factor K

in Eq. (14). Investigators at the IIT Research Institute[12] have found it necessary to use the value K = 0.7 to reconcile computed pressure rises in small models with those measured; Curves D in Figures E-4 and E-5 have been produced by a calculation based on Eq. (13), with K = 0.7 during inflow and K = 1.00 during outflow.

The value of the discharge coefficient is usually discussed in connection with boundary layer thickness and the Reynolds number.[13] It should be noted therefore that the relatively good agreement between the observed room pressures and Curves D was obtained in very small models and not in full-sized rooms. To provide an estimate of the influence of the value of K on calculated pressure rise, Curve G, based on the value K = 1.00 during both outflow and inflow, has been entered in Figure E-4. In the flow into full-sized rooms, presumably, the Reynolds number will be larger and the discharge coefficient more nearly equal to 1.00 than in the flow into small models.

Finally, the pressure increment during the interval Δt is found by substitution of Eq. (14) into Eq. (12):

$$P_3 - P_3' = K \gamma P_1 \left[\frac{2\gamma}{\gamma-1} \cdot \frac{P_1}{\rho_1}\right]^{\frac{1}{2}} \left(\frac{P_3'}{P_1}\right)^{\frac{1}{\gamma}} \left[1 - \left(\frac{P_3'}{P_1}\right)^{1-\frac{1}{\gamma}}\right]^{\frac{1}{2}} \frac{A_2 \Delta t}{V_3} \qquad (15)$$

Melichar[11,12] omits both the factors K and γ before the right-hand side of Eq. (15), which is equivalent numerically to making K = 0.7 and γ = 1.4. He attempts to justify this procedure on theoretical grounds unconnected with boundary layer theory.[12] Some of his numerical results are shown as Curves C in Figures E-4, E-5, E-6, and E-8. Melichar employs a value of Δt equal to the transit time of sound across the room.

Pursuing the analogy between room filling and steady flow into a chamber held at constant pressure, we expect to encounter the phenomenon of choking as the ratio of room pressure to outside pressure drops below the critical value.[13] For a given set of reservoir conditions, i.e., for each pair of values P_1 and ρ_1, the critical pressure ratio is that for which isentropic flow into the room achieves the maximum mass rate and for which the flow speed equals local sound speed. Therefore, to find this critical ratio, we can differentiate Eq. (14) with respect to P_3'/P_1, set the result equal to zero and solve for $(P_3'/P_1)_{crit.}$, which yields;

$$\left(\frac{P_3'}{P_1}\right)_{crit.} = \left(\frac{2}{\gamma+1}\right)^{\frac{\gamma}{\gamma-1}}$$

For every value of P_3' below the critical value as given above, mass flow into the room will be that obtained by substituting the critical ratio into Eq. (14), i.e.:

$$(\Delta m)_{choked} = K\left[\gamma\ \rho_1\ P_1\left(\frac{2}{\gamma+1}\right)^{\frac{\gamma+1}{\gamma-1}}\right]^{\frac{1}{2}} A_2\ \Delta t$$

Because the mass flow rate is limited in this way independently of the value of P_3' it is called "choked" flow. Flow obeying Eq. (14) is called "unchoked" or "subsonic." Numerically, when $\gamma = 1.4$ the critical ratio equals 0.5283; thus, assuming ambient pressure is 14.7 psia,* the critical outside pressure is

$$\frac{14.7}{0.5283} = 27.83 \text{ psia or } 13.13 \text{ psig}^{\dagger}$$

Peak overpressure in none of the experiments reported in Figures E-4, E-5, and E-6 rose above 13.13 psig; hence, according to the foregoing theory, choked flow should not have occurred.

A similar degree of comparison between calculation and measurement is found in the results shown in Figure E-8 stemming from a 27 ft^3 model exposed to a large chemical explosion, except that the transient fluctuations associated with the entering shock front are more easily discerned in the larger model than in the small shock tube models. The parameter values used in the calculations summarized in Figure E-8 were:

$P_o = 13.58$ psia	ambient pressure
$\rho_o = 0.0672$ lb/ft^3	ambient density
$\gamma = 1.4$	ratio of specific heats
$A_2 = 0.821$ ft^2	area of opening
$V_3 = 27.0$ ft^3	volume of model room

The fraction of the impacted wall area occupied by the opening is slightly less than one-tenth.

From the results shown in Figures E-4, E-5, E-6, and E-8, some estimate can be made of the validity of the greatly simplified method of computing pressure rise in a filling room set forth in Section IIA. In each figure, the value of V/2A in feet has been entered. A constant pressure

---

* Pounds per square inch, absolute.

† Pounds per square inch, gauge.

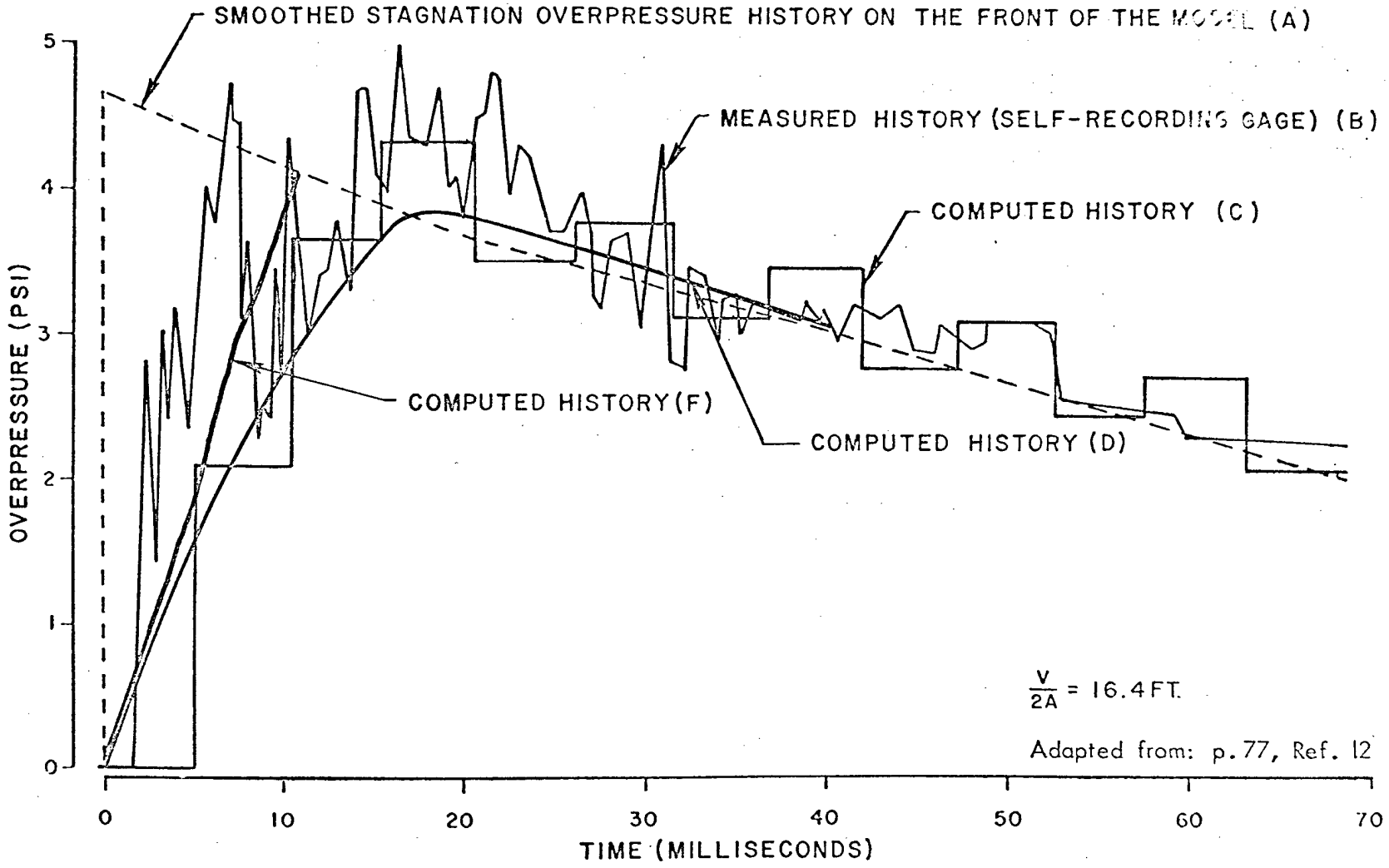

FIGURE E-8 COMPARISON OF THE COMPUTED VERSUS THE EXPERIMENTAL FILL HISTORY OF THE MODELED CHAMBER TESTED IN PROJECT DISTANT PLANE

rise from zero time and zero overpressure to a pressure equal to outside pressure at a time equal to V/2A msec overestimates the fill pressure and underestimates the fill time in the small models but seems to give results in good agreement with both calculation and measurement in the three-foot cube model reported in Figure E-8, although the presence of important oscillations (caused by shock waves) in the pressure record in the large model makes clear assessment difficult. It should be noted also that the fraction of the wall struck by the blast that is occupied by the opening (opening fraction) is over 9 percent in the large model while only 1.2 percent in the small four-in. cube models. The straight line estimate explained in Section IIA would appear to be good also in Figure E-4 for which model size is intermediate and opening fraction is almost 6 percent.

The data from the models suggest that the simplified method of estimating pressure rise in a room set forth in Section IIA is adequate when outside pressure decay is slow as in a free-field nuclear blast wave. As will be noted later, when there exists an important diffraction phase in the blast wave interaction with the structure, more sophisticated methods may be justified.

2. Outflow. All the experimental records discussed so far show that room pressure eventually exceeds outside pressure by a small amount. If all openings are into the same outside pressure field and if the fall of outside pressure is steady and slow, this overshoot is not likely to be of practical importance. However, as will be seen later, if a room has openings that are affected by different outside pressure histories, a significant outward pressure may develop on one or more walls of the room. To calculate this pressure, the rate of outflow of air through each opening must be found.

To compute inflow we treated the exterior atmosphere and the aperture leading into the room as parts of a system of ducts through which quasi-steady flow was maintained. Pressure increase within the room was computed as resulting from the transfer of mass and energy from the large outside reservoir into the room. Outflow may be treated in the same way, except that the direction of flow is opposite. For outflow, Eqs. (1) and (2) still apply, but the air in the duct now originates in the room and the adiabatic expansion law, Eq. (3), must be replaced by

$$\rho_2 = \rho'_3 \left[\frac{P_2}{P'_3}\right]^{\frac{1}{\gamma}} \tag{16}$$

Equations (1), (2), and (16) may be combined to form an equation identical to Eq. (5) except that now

$$B = \frac{2\gamma}{\gamma+1} \cdot \frac{\rho'_3}{\rho_1} \left[\frac{P_1}{P'_3}\right]^{\frac{1}{\gamma}}$$

But, as before, $y = \frac{P_2}{P_1}$ and $A = \frac{\gamma - 1}{\gamma + 1}$

In this form, Equation (5) has two solutions in the range $1 > y > 0$ whenever $\gamma = 1.4$ and

$$\frac{\rho_3'}{\rho_1} \left[\frac{P_1}{P_3'}\right]^{\frac{1}{\gamma}} > 1$$

or,

$$\frac{P_1}{\rho_1^{\gamma}} > \frac{P_3'}{\rho_3'^{\gamma}} \qquad (17)$$

These two solutions merge into a single solution at $y = \left[\frac{B}{\gamma}\right]^{\frac{\gamma}{\gamma - 1}}$

if

$$\frac{P_1}{\rho_1^{\gamma}} = (0.9094) \frac{P_3'}{\rho_3'^{\gamma}}$$

Furthermore, if $\gamma = 1.4$, Equation (5) has two solutions but only one in the range of $0 \leq y \leq 1$ whenever

$$\frac{P_3'}{\rho_3'^{\gamma}} \geq \frac{P_1}{\rho_1^{\gamma}} > (0.9094) \frac{P_3'}{\rho_3'^{\gamma}} \qquad (18)$$

Whenever

$$\frac{P_1}{\rho_1^{\gamma}} < (0.9094) \frac{P_3'}{\rho_3'^{\gamma}} \qquad (19)$$

no solution to Equation (5) exists.

Since the quantity $\frac{P}{\rho^{\gamma}}$ is constant along an isentrope and increases with entropy, when Inequality (17) is true during outflow, specific entropy outside is greater than or equal to specific entropy within the room.

The specific entropy (i.e., entropy per unit mass) in the room at any time during filling can be formally calculated as follows.

First we note that temperature of air in the room rises during the whole inflow period, as can be seen by treating Δm as a true differential and writing Equation (12) as:

$$dP_3 = \frac{\gamma P_1}{\rho_1 V_3} \cdot dm$$

From the perfect gas law

$$P_3 V_3 = m_3 R T_3$$

(where m_3 is the mass of air in the room, and R the gas constant for air) we write

$$dP_3 = \frac{R T_3}{V_3} \cdot dm + \frac{m_3 R}{V_3} \cdot dT_3$$

$$dP_3 = \frac{P_3}{m_3} \cdot dm + \frac{m_3 R}{V_3} \cdot dT_3 = \frac{\gamma P_1}{\rho_1 V_3} \cdot dm$$

$$\frac{1}{V_3}\left[\frac{\gamma P_1}{\rho_1} - \frac{P_3}{\rho_3}\right] dm = \frac{m_3 R}{V_3} \cdot dT_3$$

or

$$\left[\gamma T_1 - T_3\right] dm = m_3 \, dT_3 \qquad (20)$$

Clearly, at the start of filling $T_1 > T_3$, hence at the start $dT_3 > 0$. Moreover Equation (20) shows that T_3 can increase above T_1 while $dm > 0$ until T_3 approaches γT_1. Thus as temperature outside (T_1) falls due to the adiabatic relaxation behind the shock front, inflow and rising inside temperature continue.

In an isentropic process involving a certain mass of ideal gas the quantity $\frac{\rho}{T^{1/(\gamma - 1)}}$ is constant; or, taking differentials,

$$\frac{d\rho}{\rho} = \frac{dT}{\gamma T - T}$$

Rewriting Equation (20) as

$$\frac{dm}{m_3} = \frac{dT_3}{\gamma T_1 - T_3}$$

and dividing numerator and denominator by V_3 and noting that density $\rho_3 = \frac{m_3}{V_3}$, we find

$$\frac{d\rho_3}{\rho_3} = \frac{dT_3}{\gamma T_1 - T_3}$$

In other words the process of room filling during the time period t to t + dt results in a temperature increase dT_3 that bears the relation

$$\frac{dT_3}{(dT_3)_{isentropic}} = \frac{\gamma T_1 - T_3}{\gamma T_3 - T_3}$$

to the temperature increase in an isentropic process providing the same density increase. When $T_1 > T_3$, $\frac{dT_3}{(dT_3)_{isentropic}} > 1$

Now the entropy change dS in a process at constant density is

$$dS = \frac{c_v dT}{T}$$

where c_v is specific heat at constant volume. If we imagine a return to the isentrope (after an increment of filling) by a process at constant density or volume, the specific entropy change within the room resulting from the filling increment becomes

$$dS_3 = \frac{c_v}{T_3} \left[dT_3 - (dT_3)_{isentropic} \right]$$

or,

$$dS_3 = \frac{c_v \gamma}{T_3} \left[\frac{T_1 - T_3}{\gamma T_1 - T_3} \right] dT_3 \qquad (21)$$

which on substitution of the quantity dT_3 from Eq. (20) becomes

$$dS_3 = \frac{c_v \gamma}{T_3 m_3} (T_1 - T_3) dm \qquad (22)$$

Therefore, during inflow (i.e., when $dm > 0$) specific entropy within the room will increase until $T_3 = T_1$ or $P_3 = P_1$, whichever occurs first.

Because of the passage of the shock front, air outside has greater than ambient specific entropy. Hence, initially before inflow begins

$$\frac{P_1}{\rho_1^{\gamma}} > \frac{P_3}{\rho_3^{\gamma}}$$

but Eq. (22) shows that the inflow process, according to the theory applied here, creates entropy within the room. Should enough entropy be so created, Inequality (19) may eventually be satisfied and solution of the outflow equations presented here may be impossible. The rise in specific entropy within the room as a result of inflow is:

$$\Delta S_3 = c_v \gamma \int_{t=0}^{P_3=P_1} \frac{T_1 - T_3}{T_3 m_3} \frac{dm}{dt}\, dt$$

where t = time and T_1, T_3, and m_3 are functions of time. From Eq. (20) we know that T_3 rises asymptotically toward γT_1 until $P_1 = P_3$; thus T_3 may be larger than T_1. For a given function $P_1(t)$ [which determines $T_1(t)$, $T_3(t)$, and $m_3(t)$], the maximum specific entropy within the room will be reached when

$$T_3 = T_1$$

If we assume that at this time inflow is still under way, then

$$P_1 > P_3$$

which implies, when $\gamma > 1$, that

$$P_1^{1-\frac{1}{\gamma}} > P_3^{1-\frac{1}{\gamma}}$$

or

$$P_1^{\frac{1}{\gamma}-1} < P_3^{\frac{1}{\gamma}-1}$$

Now from the equality of the temperatures at this time, the perfect gas law implies

$$\frac{P_1}{\rho_1} = \frac{P_3}{\rho_3}$$

Multiplying both sides by the last inequality above, we find

$$\frac{P_1^{\frac{1}{\gamma}}}{\rho_1} < \frac{P_3^{\frac{1}{\gamma}}}{\rho_3}$$

or

$$\frac{P_1}{\rho_1^{\gamma}} < \frac{P_3}{\rho_3^{\gamma}}$$

Hence, in general, the possibility may not be ruled out that Inequality (19) will be satisfied. Whether the outflow equations as presented here have a solution will depend on the nature of the function $P_1(t)$. If outflow is to be calculated, then to provide an initial disparity between specific entropy outside and inside, the inflow period must be treated using the initial density behind the shock front and computed from the Hugoniot relation:[1]

$$\rho_{1o} = \rho_o \frac{(\gamma+1)P_{1o} + (\gamma-1)P_o}{(\gamma-1)P_{1o} + (\gamma+1)P_o} \tag{23}$$

Subsequent outside air densities may be calculated from the adiabatic law:

$$\rho_1 = \rho_{1o}\left[\frac{P_1}{P_{1o}}\right]^{\frac{1}{\gamma}} \tag{24}$$

In Eqs. (23) and (24), ρ_{1o} and P_{1o} refer to the air density and absolute pressure immediately behind the shock front. When peak pressure at an opening is reached by reflection of an incident shock wave from a wall, Eq. (24) is not correct regardless of whether P_{1o} is taken as peak incident absolute pressure or peak reflected absolute pressure, but the error in using Eq. (24) is small. We will arbitrarily consider ρ_{1o} and P_{1o} as representing conditions behind the free-field shock front. Use of Eqs. (23) and (24) may make it possible to satisfy the reverse of Inequality (19).

Should such still not be possible, other calculational methods must be used for the outflow phase, such as that proposed by Melichar[11,12] or that reported by IIT Research Institute.[17] These methods equate duct pressure P_2 with outside pressure during outflow; the IIT investigators then fit observed outflow pressure data by choosing values for the discharge coefficient and for the ratio of inside to outside pressure at the time of flow reversal.

3. Outline of Hand Calculation. In constructing from the foregoing equations a calculational scheme for estimating the parameters of flow into and out of a single room with a single opening we start with a series of values of P_1, one for each time step. These may be obtained by linear interpolation from a given table of outside pressure as a function of time and each value should pertain to the center of the time interval. The size of the time interval, Δt, itself is arbitrary, but it should be no greater than the quantity τ; presumably up to a limit, greater accuracy results from smaller values of Δt. The size of Δt may be changed during the calculation when the rate of change of flow parameters changes. We also need values for ambient pressure P_o and density ρ_o.

Two methods of calculation are shown below. The first is that used to produce Curves F in Figures E-4, E-5, E-6, and E-8, namely, that based on Eqs. (1), (2) and (3) for inflow or Eqs. (1), (2) and (24) for outflow, and in the outline below it is called Method F. This method has the advantage of great simplicity and of not requiring knowledge of empirical constants; however, as will be explained later, values of wind speed and dynamic pressure computed by it are subject to doubt in some cases and for that reason a method given by IIT Research Institute is included also. The latter method is responsible for Curves D in the figures and, therefore, in the outline below it is called Method D. As noted earlier, Method D for the unchoked flow case is numerically equivalent to the calculation used by Melichar.[11,12]

Average pressure inside a room and dynamic pressure in the single opening to an outside reservoir whose pressure variation in time is known may be calculated as functions of time by the sequential application of the steps stated below. Each cycle through a series of steps completes the calculation for one time interval. The first three steps are executed only during the first cycle; subsequent passes begin with step (4), as indicated in the outline. Step (5) is a branch point to separate sequences for inflow and outflow, chosen according to a criterion given in step (5). There are further branches (a) to Method D or F, chosen at the discretion of the user at each time, and (b) under Method D to choked or unchoked flow, determined by stated criteria. Throughout the outline, the quantity γ has been set equal to 1.4.

(1) Set $P'_3 = P_o$ and $\rho'_3 = \rho_o$ and $t = 0$.

(2) Compute

$$\rho_{1o} = \rho_o \frac{6P_{1o} + P_o}{P_{1o} + 6P_o}$$

where P_{1o} is the absolute pressure immediately behind the shock front.

(3) Choose value of Δt (see opening paragraph of this Section IIB3).

(4) Determine outside pressure at the current time; i.e., determine P_1, from the known reservoir pressure history (pressure variation with time). During first time interval $P_1 = P_{1o}$.

(5) Determine direction of flow; i.e., if $P_1 > P_3'$, flow is inward; go to step (6). Otherwise flow is outward; go to step (28).

Inflow

(6) Compute

$$\rho_1 = \rho_{1o}\left[\frac{P_1}{P_{1o}}\right]^{0.7143}$$

Branch to selected Method below for step number (7D) (Method D) or step (7F) (Method F).

Method D (Inflow)

(7D) If $P_3'/P_1 \leq 0.5283$ inflow is choked; go to step (8D). Otherwise inflow is unchoked; go to step (18D).

Choked Inflow

(8D) $$\Delta m_{choked} = K\left[1.4\,\rho_1 P_1 \left(\frac{2}{2.4}\right)^{\frac{2.4}{0.4}} F^*\right]^{1/2} A_2\,\Delta t$$

$$= 0.6847\,K\,[\rho_1 P_1 F]^{1/2} A_2\,\Delta t$$

Using the recommended value[17] of K = 0.70 this becomes

$$\Delta m_{choked} = 0.4793\,[\rho_1 P_1 F]^{1/2} A_2\,\Delta t$$

(9D) $$P_2 = P_3'$$

(10D) $$\rho_2 = \rho_1\left[\frac{P_2}{P_1}\right]^{0.7143}$$

---

* The factor F will often be necessary for consistency of units. For example, if u_2 is to be in ft/sec and P_1 is in lb/in^2 and ρ_1 in lb/ft^3, then F = 32. X 144. = 4,608.

(11D) $$u_2 = \frac{\Delta m_{choked}}{\Delta t\, A_2 \rho_2 K}$$

(12D) $$P_3 = P_3' + 1.4 \frac{P_1}{\rho_1} \frac{\Delta m}{V_3}$$

If desired, dynamic pressure q_2 at the opening may be found from:

(13D) $$q_2 = \frac{1}{2} \frac{\rho_2 u_2^2}{F}$$

(14D) $$\rho_3' = \rho_3$$

(15D) $$P_3' = P_3$$

(16D) Advance time by amount Δt and return to step (4).

Unchoked Inflow

(18D) $$P_2 = P_3'$$

(19D) $$\rho_2 = \rho_1 \left[\frac{P_2}{P_1}\right]^{0.7143}$$

(20D) $$u_2^2 = 7 \left[\frac{P_1}{\rho_1} - \frac{P_2}{\rho_2}\right] F$$

(21D) $$\Delta m_{unchoked} = \rho_2 u_2 A_2 \Delta t$$

(22D) $$P_3 = P_3' + 1.4 \frac{P_1}{\rho_1} \frac{\Delta m_{unchoked}}{V_3}$$

(23D) $$\rho_3 = \rho_3' + \frac{\Delta m_{unchoked}}{V_3}$$

(24D) If desired, dynamic pressure, q_2, in the opening may be found from:

$$q_2 = \frac{1}{2} \rho_2 \frac{u_2^2}{F}$$

(25D) $P_3' = P_3$

(26D) $\rho_3' = \rho_3$

(27D) Advance time by amount Δt and return to step (4).

Method F (Inflow)

(7F) $P_2 = 0.1912\ P_1$

(8F) $\rho_2 = \rho_1 \left[\frac{P_2}{P_1}\right]^{0.7143} = 0.3067\ \rho_1$

(9F) $u_2^2 = 7 \left[\frac{P_1}{\rho_1} - \frac{P_2}{\rho_2}\right] F = 2.637 \left[\frac{P_1}{\rho_1}\right] F$

(10F) $\Delta m_3 = u_2\ \rho_2\ A_2\ \Delta t = 0.498\ (P_1\ \rho_1\ F)^{1/2}\ A_2 \Delta t$

(11F) $P_3 = P_3' + 1.4\ \frac{P_1}{\rho_1}\ \frac{\Delta m_3}{V_3}$

(12F) $\rho_3 = \rho_3' + \frac{\Delta m_3}{V_3}$

(13F) If desired, the dynamic pressure, q_2, in the doorway may be calculated:

(14F) $q_2 = \frac{1}{2}\ \rho_2\ \frac{u_2^2}{F} = 0.4044\ P_1$

(15F) $\rho_3' = \rho_3$

(16F) $P_3' = P_3$

(17F) Advance time by amount Δt and return to step (4).

Outflow

(28) Branch to selected Method below for step (29D) (Method D) or step (29F) (Method F).

Method D (Outflow)

(29D) If $P_1/P_3' \leq 0.5283$, outflow is choked; go to step (30D). Otherwise outflow is unchoked; go to step (39D).

Choked Outflow

(30D) $$\Delta m_{choked} = -0.6847\ K\ [\rho_3' P_3' F]^{1/2}\ A_2 \Delta t$$

For K = 1.0 this becomes[17]

$$\Delta m_{choked} = -0.6847\ [\rho_3' P_3' F]^{1/2}\ A_2 \Delta t$$

(31D) $$P_2 = P_1$$

(32D) $$\rho_2 = \rho_3' \left[\frac{P_2}{P_1}\right]^{0.7143}$$

(33D) $$u_2 = \frac{\Delta m_{choked}}{\Delta t\ A_2\ \rho_2\ K}$$

(34D) $$P_3 = P_3' + 1.4\ \frac{\Delta m_{choked}}{V_3}\ \frac{P_3'}{\rho_3'}$$

(35D) $$\rho_3 = \rho_3' + \frac{\Delta m}{V_3}$$

(36D) $$P_3' = P_3$$

(37D) $$\rho_3' = \rho_3$$

(38D) Advance time by amount Δt and return to step (4)

Unchoked Outflow

(39D) $$P_2 = P_1$$

(40D) $$\rho_2 = \rho_3' \left[\frac{P_2}{P_3'}\right]^{0.7143}$$

(41D) $$u_2^2 = 7 \left[\frac{P_1}{\rho_1} - \frac{P_2}{\rho_2}\right] F$$

(42D) $\Delta m_{unchoked} = -\rho_2 u_2 A_2 \Delta t$

(43D) $P_3 = P'_3 + 1.4 \frac{\Delta m_{unchoked}}{V_3} \frac{P'_3}{\rho'_3}$

(44D) $\rho_3 = \rho'_3 + \frac{\Delta m_{unchoked}}{V_3}$

(45D) $P'_3 = P_3$

(46D) $\rho'_3 = \rho_3$

(47D) Advance time by amount Δt and return to step (4).

Method F (Outflow)

(29F) $B = \frac{7}{6} \frac{\rho'_3}{\rho_1} \left[\frac{P'_3}{P_1} \right]^{0.7143}$

(30F) Solve $By^{0.7143} = y + A$ for y.

(31F) $P_2 = yP_1$

(32F) $\rho_2 = \rho'_3 \left[\frac{P_2}{P'_3} \right]^{0.7143}$

(33F) $\Delta m = -\rho_2 u_2 A_2 \Delta t$

(34F) $P_3 = P'_3 + 1.4 \frac{P_1}{\rho_1} \frac{\Delta m}{V_3}$

(35F $\rho_3 = \rho'_3 + \frac{\Delta m}{V_3}$

(36F) $P'_3 = P_3$

(37F) $\rho'_3 = \rho_3$

(38F) Advance time by amount Δt and return to step (4).

The theoretical differences between the two methods outlined above are striking. At the present time there is not enough experimental evidence from full-sized rooms to permit a clear judgment between them. If the room fills slowly, that is, the filling time is long compared with the transit time of sound across the room, then the analogy underlying Method D should be good; but even so there is doubt about the correct value of the discharge coefficient, K. The possible influence of K on the calculated room pressure is large, as can be seen from the difference between Curves D and G in Figure E-4. If the filling is rapid, perhaps Method F should be preferred. However, as will be seen in the following paragraphs, this Method can lead to anomalous values of wind speed through the opening.

C. Wind Speed and Dynamic Pressure (Jet Effect)

Other flow parameters of interest are wind speed and dynamic pressure. The present simple methods yield values of these parameters only in the doorway, but, ordinarily, values at the doorway may serve as upper bounds for the whole room.

Unfortunately, measurements of wind speed and dynamic pressures in shock-filling rooms are even fewer than observations of room pressure. The differences among the predictions of speed among the several calculational methods are large, but the values of dynamic pressure are often in fair agreement. For estimates of the acceleration of objects in the stream, the dynamic pressure is the only pertinent parameter.

During both inflow and outflow wind speed may be calculated from Eq. (9) and, if the isentropic assumption is made, Eq. (6). Dynamic pressure, q_2, is customarily defined as

$$q_2 = \frac{1}{2} \rho_2 u_2^2$$

Using Eq. (9) this can be written:

$$q_2 = \frac{1}{2} \quad P_1 \quad (1 - y_o) \qquad (25)$$

Because of the neglect of transient effects, Eqs. (9) and (25) do not reflect the influence of changes in the room pressure, and values calculated from them may be unrealistic. Peak speeds found from Eq. (9) for the experiments reported in Figures E-4, E-5, E-6, and E-8 are supersonic, i.e., above local sound speed in the doorway.

Because of its use of the choking analogy Method D never calculates supersonic speeds; but it does neglect transient shock fronts which could alter the flow substantially in fast filling rooms.

Table E-1 contains the several calculated values of peak speed and dynamic pressure corresponding to each of the experiments reported in Figures E-4, E-5, E-6, and E-8. The table suggests that use of Method F may result in overestimate of that important criterion for damage potential, dynamic pressure. As noted above, because signals from the filling room into the outside reservoir are neglected, Method F in addition to overestimating peak dynamic pressure may overestimate the time-average dynamic pressure in the doorway.

There are no direct observations of wind speed in the opening to compare with calculations. Coulter,[9] however, had reported (1) measurements of the acceleration of an $\frac{1}{8}$-inch diameter nylon ball placed in the doorway of a small model struck head-on by a weak shock wave, and (2) measurements of the motion of smoke columns inside these models during shock filling. With the help of acceleration coefficients derived (theoretically and experimentally) by Bowen and others[14] we can compute motion of the nylon sphere from Eq. (25). Coulter allowed a shock front of overpressure equal to 4.89 psig to strike a reflecting plate in which an entrance 1 x 4 inches was cut. Since the chamber behind the opening had a volume to opening area ratio (V/A) equal to 1.33, filling was essentially complete in 1.33/2 = 0.667 ms, during which time there was little or no decay of the incident wave. If we assume ambient pressure equal to 14.7 psi, reflection at

Table E-1

PEAK VALUES OF OTHER FLOW PARAMETERS

Method / Experiment	C*		F		G	
	q_2(psi)	u_2(fps)	q_2	u_2	q_2	u_2
Fig. E-4	7.98	1045.	9.93	1650.	8.02	985.
Fig. E-5	10.2	1180.	11.2	1680.	10.2	1110.
Fig. E-6	7.79	972.	9.74	1640.	7.80	972.
Fig. E-8	4.08	747.	7.37	1634.		

* Correct adiabatic law has been substituted for the inverted form appearing in Melichar's FORAST code.[11]

normal incidence of a 4.89 psi shock produces a reflected overpressure equal to 11.1 psi.[1] Hence the value of P_1 in Eq. (25) becomes 11.1 + 14.7 = 25.8 psi, and

$$q_2 = \frac{1}{2} \times 25.8 \ (1 - 0.1912)$$

$$= 10.5 \text{ psi}$$

or

$$q_2 = 48100 \text{ lb/sec}^2 \text{ ft}$$

In this expression "lb" is a unit of mass.

A still object in a stream of moving air is accelerated according to the formula

$$\frac{dv}{dt} = \alpha \, q \qquad (26)$$

where α is an acceleration coefficient characteristic of the object and q is the dynamic pressure as defined here. Eq. (26) continues to hold for the moving object as long as its speed is small compared to air speed. Bowen and others[14] suggest a value of $\alpha = 0.138$ ft^2/lb for a 1/8 inch diameter steel sphere. Since α is inversely proportional to mass, the corresponding value for a nylon sphere of the same size is approximately

$7.87 \times 0.138 = 1.09$ ft^2/lb (specific gravity of iron equals 7.87). Hence acceleration of the nylon sphere should be, according to Eq. (26),

$$\frac{dv}{dt} = 1.09 \times 48100 = 52200 \text{ ft/sec}^2$$

and the final speed of the sphere when filling is complete 667 μsec after impact becomes:

$$v = 52200 \times 667 \times 10^{-6} = 34.8 \text{ ft/sec}$$

and the displacement is $s = \frac{1}{2} \times 52200 \times (667)^2 \times 10^{-12} = 0.0116$ ft = 0.14 inch. Coulter measured terminal speed after 700 μsec as 29.8 ft/sec. Observed displacement in this same time was approximately 0.10 inch, which means the ball did not move far from the center of the doorway during the period of observation and was subjected to only slightly attenuated peak dynamic pressure.

Corresponding to Eq. (25), Method D produces the following equation for the calculation of dynamic pressure in the opening:

$$q_2 = \frac{7}{2} P_1 \left[\left(\frac{P_3'}{P_1} \right)^{\frac{1}{\gamma}} - \frac{P_3'}{P_1} \right] \qquad (27)$$

The value of q_2 in Eq. (27) is not constant in time even when P_1 does not change appreciably. For simplicity, we may assume P_3' varies linearly from 14.7 psia to P_1 over the filling time 0.667 ms. Again, we take $P_1 = 25.8$ psia and find the following variation of dynamic pressure with time:

time (ms)	0	0.2	0.4	0.6	0.667
P_3' (psia)	14.7	18.0	21.35	24.7	25.8
q_2 (psi)	8.97	6.80	4.15	1.08	0.00

The tabulation shows a nearly linear variation of q_2. Integrating Eq. (26) approximately, we find the final value of speed to be:

$$v = 1.09 \frac{f_t^2}{lb} \cdot \frac{1}{2} \times 8.97 \frac{lb}{in^2} \; 0.667 \times 10^{-3} \; sec \; 144 \frac{in^2}{ft^2} \; 32 \frac{ft}{sec^2}$$

$$= 15.0 \frac{ft}{sec}$$

which is about half the observed value. The relatively better agreement with experiment furnished by Method F than by Method D may reflect the fact that the shock filling in this case is "fast."

However, it would seem that any relatively good agreement between calculated and observed acceleration in this example was fortuitous, since Coulter's photographs of events in the chamber make it clear that the diffraction episode very nearly coincided with the calculated filling time, that is, air flow during the period of observation was more a shock related process than a case of quasi-steady adiabatic flow. Some support for this view comes from the second set of wind observations reported by Coulter: motion of smoke in the same kind of chamber used for measurements of the motion of the nylon ball. Most of Coulter's observed values of wind speed and dynamic pressure from smoke motion are one or two orders of magnitude lower than comparable values calculated by the methods presented here. However, Coulter could not by this smoke method measure speeds in the doorway and, in fact, as filling went on his observations were restricted to regions farther and farther from the core of the flow.

To provide a useful appraisal of the effects of inflowing air within an open shelter, the attenuation of wind speed and the spreading of the jet as the influx moves through the entry deeper into the enclosure must be accounted for. As in our description of the average pressure rise within the room, reliance will again be placed on a quasi-static approach, with account taken of the transient episode before the establishment of adiabatic flow by means of a semiempirical correction.

The steady jet described by Abramovich[20] is illustrated in Figure E-9A where air is considered to be flowing from a reservoir at high pressure on the left through the aperture into the region of low pressure (i.e., the interior of the shelter) on the right. In the theory, the entry aperture may be a slit of essentially infinite length and width b_o or it may be a circular opening of diameter b_o. Although the description of the jet is different for the slit than for the circle, the difference is not important here. Since most actual openings will be somewhere between the two, it will be assumed that any actual opening has been approximated by a slit or by a circle and only one set of formulas will be given. As shown in Figure E-9A, inflowing air generally fans out into the receiving reservoir, slowing down after passing through a conical or wedge-shaped "core." Air speed is constant everywhere within the core.

Abramovich characterizes the jet by three parameters: dimension of the opening b_o ; air speed in the axial direction at the initial cross section u_o ; and ratio θ between temperature in the core and that in the receiving reservoir (i.e., the shelter space). The flow is driven by a pressure difference between the two reservoirs, but it appears to be a fact that pressure within the usual subsonic jet itself is uniform and equal to that in the receiving reservoir. In other words, pressure equilibrium is quickly established between the jet and the air already in the reservoir. In this case, where the air in the high pressure reservoir has been shock compressed from a state identical to that originally in the low pressure reservoir, the existence of pressure equilibrium between the inflowing air and interior air requires that density and temperature in the jet nearly equal density and temperature in the room. The slight difference is attributable to the fact that outside air has passed through the shock front and acquired entropy compared with the unshocked or only weakly shocked air within the room. Such difference is entirely negligible for present purposes. Thus, in this discussion, the parameter θ equals 1.

Furthermore, if pressure is uniform within the jet, the flux of axial momentum must be the same at each cross section of the jet, that is:

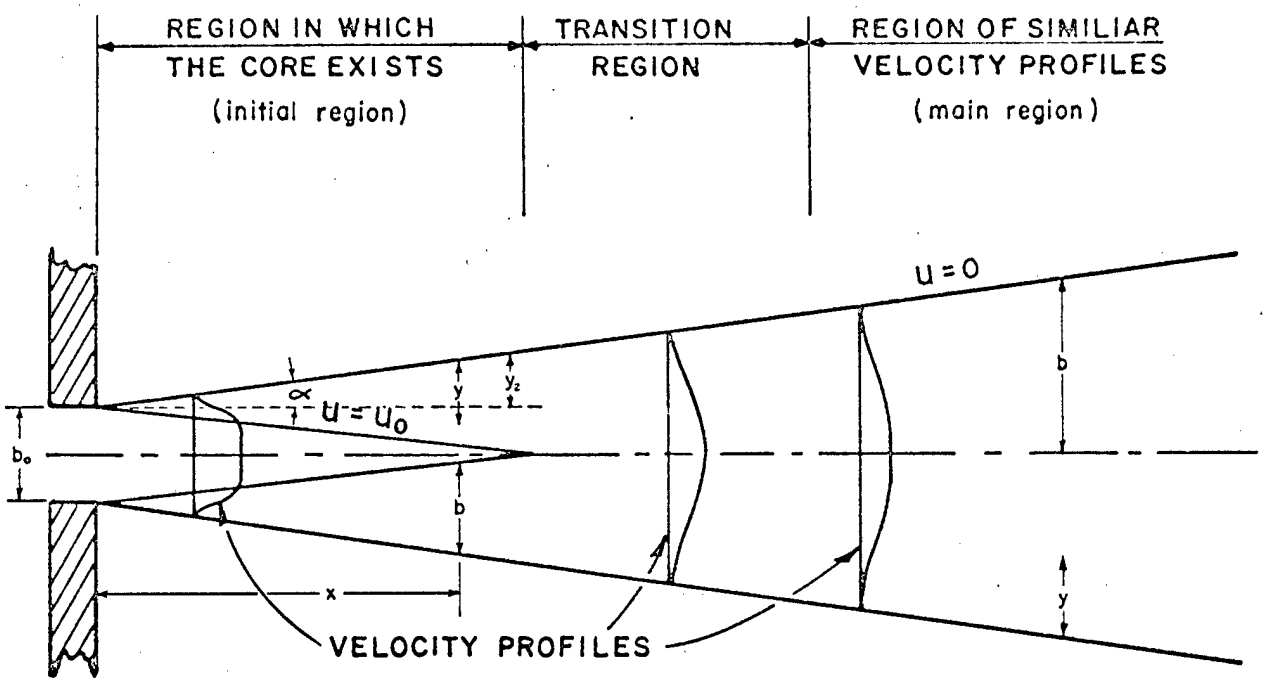

Source: Ref. 20

FIGURE E-9A SCHEMATIC OF JET FLOW

$$\text{flux} = \rho_3 u_o^2 A_2 \tag{28}$$

By making use of a control surface passing through the aperture (shown by the dashed line in Figure E-9B), the value of u_o in Equation 28 can be calculated, since by conservation of momentum

$$\text{flux} = (P_1 - P_3) A_2$$

Thus,

$$u_o = \left[\frac{P_1 - P_3}{\rho_3}\right]^{1/2} \tag{29}$$

Alternatively, by Equation 2

$$P_1 - P_2 = \rho_2 u_2^2 = 2q_2$$

or

$$P_1 = 2q_2 + P_2$$

which can be substituted for P_1 in Equation 29 to yield:

$$u_o = \left[\frac{2q_2 + P_2 - P_3}{\rho_3}\right]^{1/2} > \left[\frac{2q_2 - P_3}{\rho_3}\right]^{1/2} \tag{30}$$

This may be a useful lower bound since P_2 is generally small. Both Equations 29 and 30 show that u_o falls as the room fills.

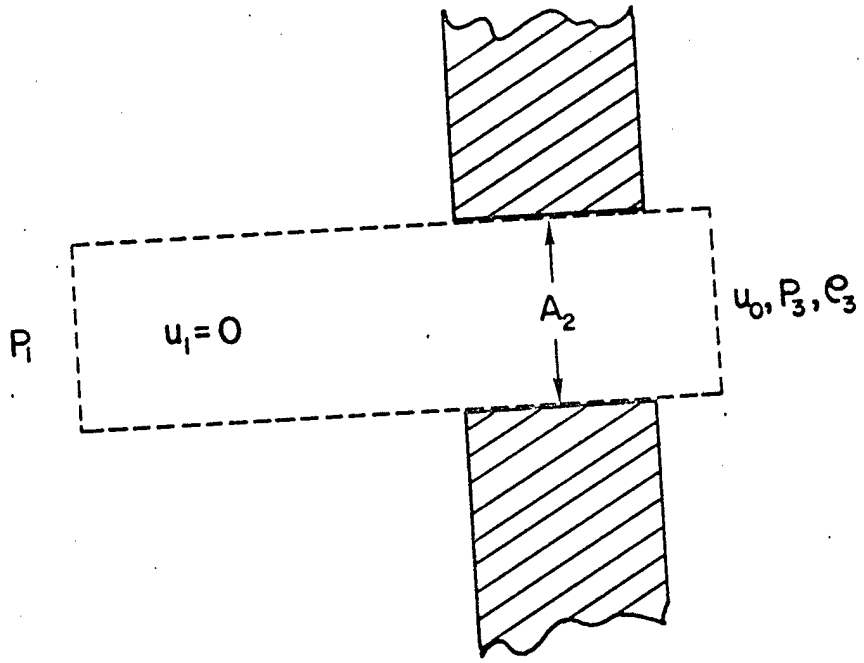

FIGURE E-9B CONTROL SURFACE FOR CALCULATION OF CORE SPEED

$$q_{core} = \frac{1}{2}\rho_3 u_o^2 = \frac{1}{2}\left[P_1 - P_3\right] = q_2 - \frac{1}{2}(P_3 - P_2) \qquad (31)$$

Experimental observations[21] in model rooms and detailed numerical simulations[21,22] of shock room filling both demonstrate that in room filling streams dynamic pressure reaches values about twice those given by Equation 31. Thus, instead of Equations 29 and 31 the following is recommended on empirical grounds:

$$u_o = \left[\frac{2(P_1 - P_3)}{\rho_3}\right]^{1/2} \qquad (32)$$

$$q_{core} = P_1 - P_3 \qquad (33)$$

In most cases the relation

$$q_{core} = q_2 \qquad (34)$$

has been found empirically to be approximately true at the beginning of the jet period. The use of Equation 34 throughout the filling period appears from experimental evidence to be highly conservative, since in addition to the spatial attenuation, observations reveal a fall in core dynamic pressure with time during the equalization of inside and outside pressures.

The reason for the failure of Equations 29 and 31 is not understood; however, with further empirical corrections, steady-state jet theory may be applied with fair success to describe the room filling airstream quantitatively.

The first departure from straightforward steady jet behavior is observed during the period immediately after shock arrival at the opening, when air motion in the neighborhood of the opening is governed by the laws of shock waves. At that time, particle speed is relatively slow

but as the diffracted waves reverberate in the opening, conditions for jet-like flow are established. This build-up of flow through the opening lasts a length of time

$$t_o \cong \frac{9b_o}{c} \tag{35}$$

where c is the speed of sound. If this time interval is long enough to be important, it is recommended that dynamic pressure in the opening be treated as varying linearly in time during t_o from $q_o = 0$ at shock arrival ($t = 0$) to $q_o = P_1 - P_3$ at the end of the diffraction phase ($t = t_o$). During the time $t < t_o$, the variation in P_3 with time cannot be calculated since the filling law during diffraction at the opening is extremely complicated. If substantial filling is thought to take place during the period $t < t_o$, the inflow rate at any time step may be found from the formula:

$$\Delta m_3 = \rho_3' u_o A_2$$

$$= A_2\left[2q_o\rho_3'\right]^{1/2} \tag{36}$$

The jet is not established simultaneously throughout its final length. An estimate of the time between shock arrival and the appearance of jet-like flow at an interior point i appears to be:

$$t_{oi} = \frac{9\ell_o}{c} \tag{37}$$

where ℓ_o is the distance from the opening to the point. Again a fair appraisal of the time variation of dynamic pressure at point i during this preliminary period would seem to be a straight line, beginning at the moment of shock arrival at point i.[21]

If the point i is near a wall blocking flow from the opening, then dynamic pressure there may never reach a value expected in a fully developed flow at that distance from the opening.

The fully developed steady subsonic jet is described by the following three sets of formulas, each set valid in one of the three regions shown in Figure E-9A. Only air speed in the axial direction is significant.

1. Initial Region. The speed u in the boundary layer outside the core decreases with increasing distance from the core. At the jet boundary u = 0 and at the core boundary u = u_o. At a point in any plane at right angles to the jet axis and within the boundary layer

$$u = u_o \left\{1 - \left[1 - \eta^{1.5}\right]2\right\}$$

where $\eta = \frac{y}{b}$, y is the distance from the jet boundary (measured in a direction perpendicular to the jet axis) to any point, and b is the boundary layer thickness also measured perpendicularly to the axis, both as shown in Figure E-9A (e.g., at the core boundary y = b and at the jet boundary y = 0). The quantity b varies linearly with distance x from the opening, i.e.,

$$b = 0.27x$$

or, equivalently, the slope of the outer jet boundary (where u = 0) can be written

$$\tan \alpha = 0.158 \quad \text{or} \quad \alpha \cong 9^\circ$$

The length of the initial region (and the length of the core) is approximately $4.5b_o$.

Transition Region. Formulas valid for the transition region can be written, but they are not necessary for present purposes. If desired, values of quantities in this region may be interpolated between the initial and main regions. The length of the transition region however may be required and is approximately $2.2b_o$.

Main Region. Here, as in the transition region, there is no core; the jet is entirely boundary layer, which widens at half angle equal to

$$\alpha \cong 12^{o}30'$$

or slope

$$\frac{b}{x} = 0.22$$

where b is now the half width of the jet.

In any cross section, air speed is at a maximum at the jet axis and falls to zero at the outer boundary. In between at a perpendicular distance $y < b$ from the axis

$$u = u_m(1 - \eta^{1.5})^2$$

where u_m = speed along the axis and $\eta = \frac{y}{b}$ as before, except that y and b have slightly different meanings, as shown in the main region of the jet sketched in Figure E-9A.

Speed along the axis u_m declines as distance from the opening increases, i.e.:

$$u_m \cong u_o \frac{6.2\ b_o}{x}$$

Hence

$$u \cong u_o \frac{6.2\ b_o}{x}(1 - \eta^{1.5})^2$$

or

$$q \cong q_{core}\left(\frac{6.2\ b_o}{x}\right)^2(1 - \eta^{1.5})^4$$

Any potential for damage residing in the airstream stems ultimately from Equation 29. Changes in the values of the thermodynamic parameters in that equation are not felt immediately and simultaneously throughout

the stream. However, the assumption of instantaneous response will fail to be conservative only after the end of inflow, i.e., when $P_1 = P_3$ and u_o as calculated by Equation 29 becomes 0. In fact, the stream cannot stop abruptly. If the airstream deep within a shelter remains dangerous as filling concludes, then a linear decay in dynamic pressure at the interior location may be assumed, lasting

$$t_1 = \frac{9\ell_o}{c}$$

or, more simply, inertial effects during decay may be accounted for by neglecting inertial effects during build-up of the stream at the interior point.

Obstacles to flow, such as corners or barriers, may be found in a shelter or may be deliberately designed into the structure. As far as the main shelter area is concerned, such entry barriers or mazes have the effect of increasing the length of the diffraction phase. Thus if the driving pressure is falling rapidly enough, the duration and/or intensity of the airstream flowing into the shelter may be reduced by the presence of a simple barrier at the entry, as sketched in Figure E-9C. Increase in the duration of the diffraction phase (i.e., the time interval t_o) is a possible explanation for the positive results of Coulter's barrier experiments.[21] However, Equations 32 and 33 appear to offer the possibility of baffles that would with a sacrifice of shelter space greatly reduce the hazard connected with the filling stream. For example, a holding room or foyer is shown in Figure E-9D that could conceivably be designed so that pressure within it during most of the fill period would be less than that present outside the shelter. If such a design is possible, Equation 33 tells us that the dynamic pressure in the core of the jet emerging into the actual shelter space would be less than it would be without the foyer. The difference between the holding rooms shown in Figures E-9D and E-9E should be noted. The driving pressure for the jet flowing into the shelter space of Figure E-9E is essentially the outside pressure, not that in the holding room. This arrangement benefits only from the increased delay t_o . The hazardous jet of Figure E-9D on the other hand is driven by the pressure in the holding room. If the foyer volume V and door areas A_1 and A_2 could be designed to keep the average pressure in V substantially below P_1 , then the arrangement would lead to reduced values of q_o after the delay t_o has elapsed.

Some of the same considerations may be used in understanding stream deflection within the shelter space, such as the situation illustrated in Figure E-9F, where the airstream flows into a corner of the shelter

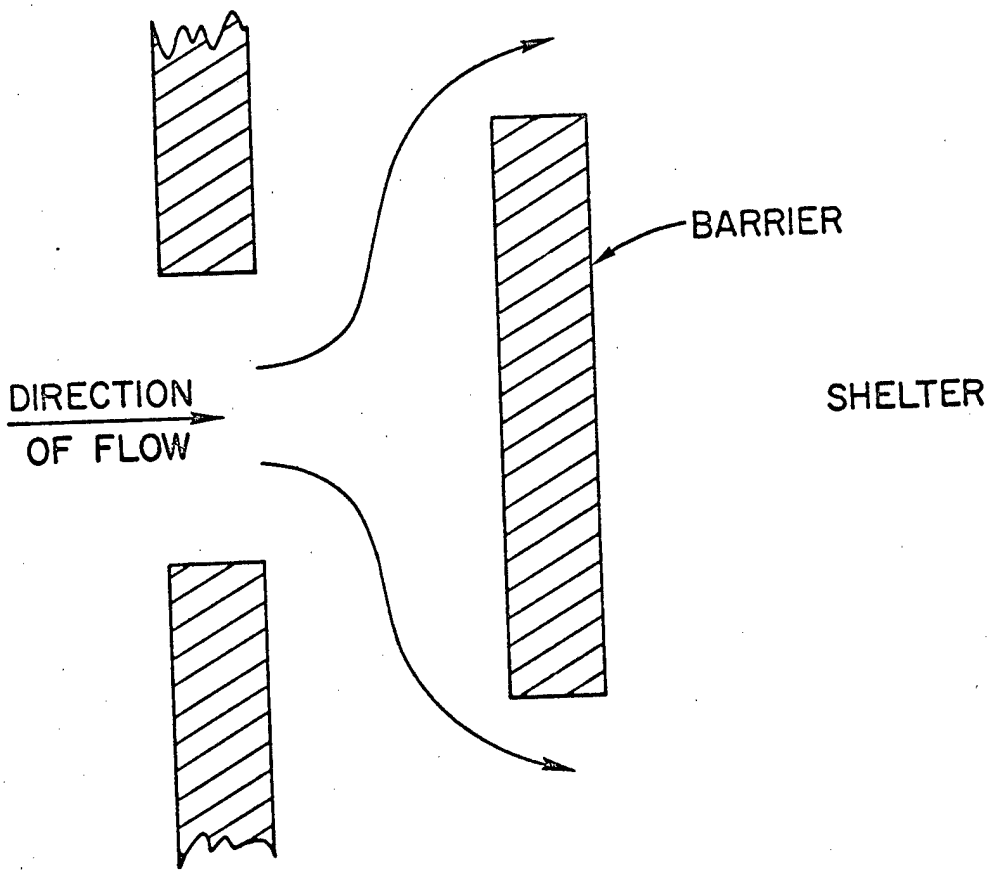

FIGURE E-9C SIMPLE BARRIER AT SHELTER ENTRY

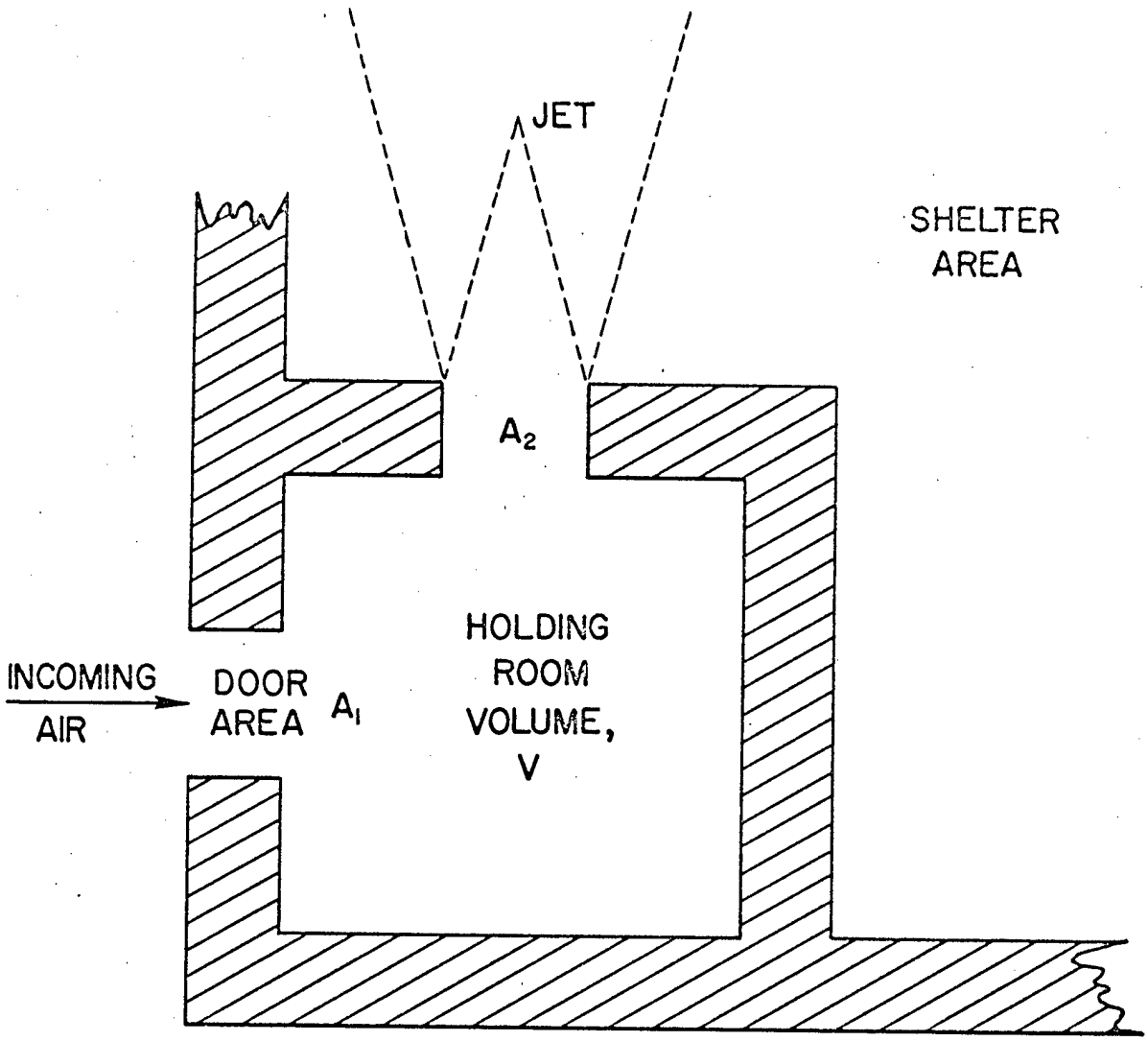

FIGURE E-9D POSSIBLE HOLDING ROOM TO REDUCE WIND HAZARD

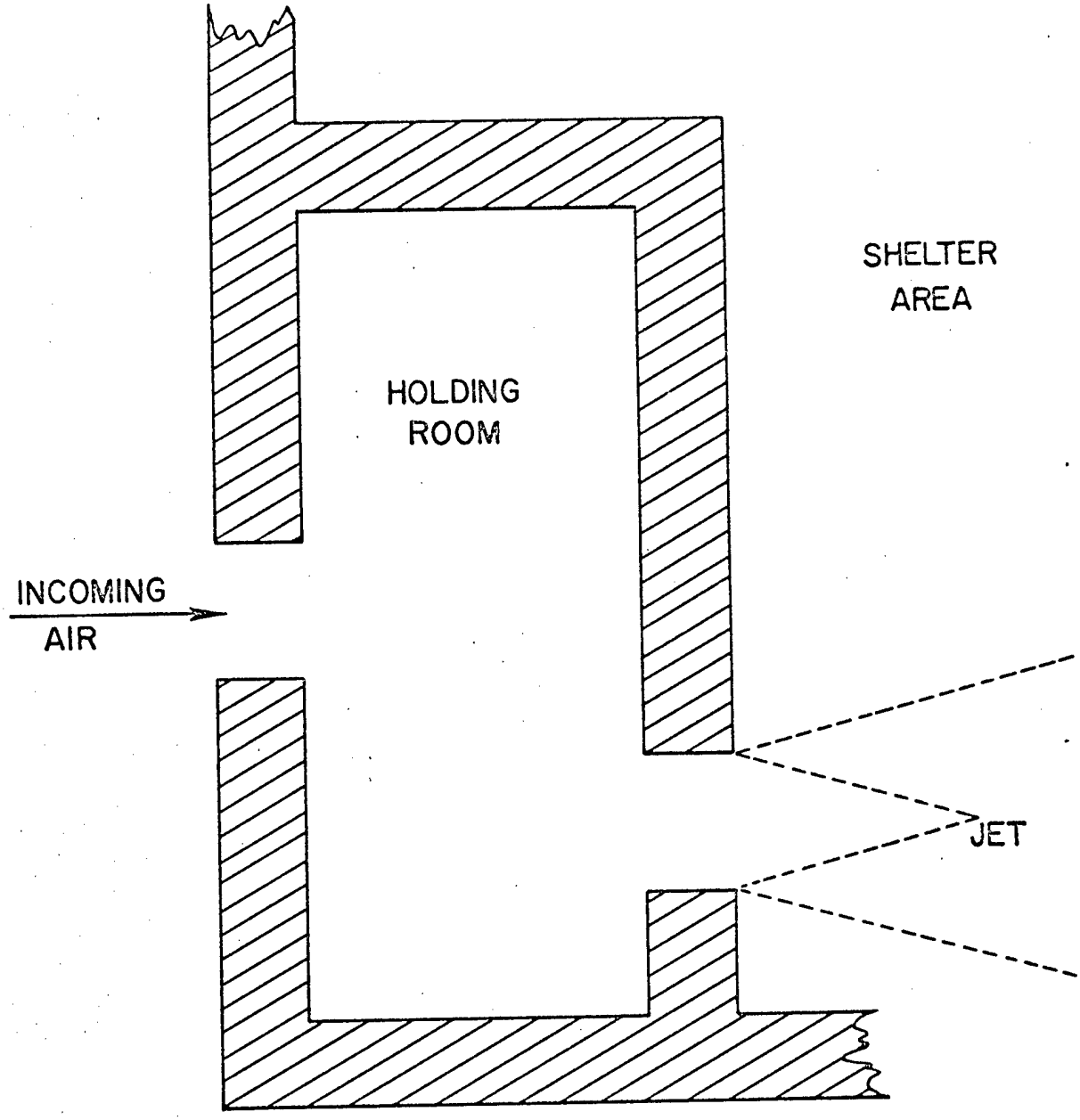

FIGURE E-9E IMPROPERLY DESIGNED HOLDING ROOM

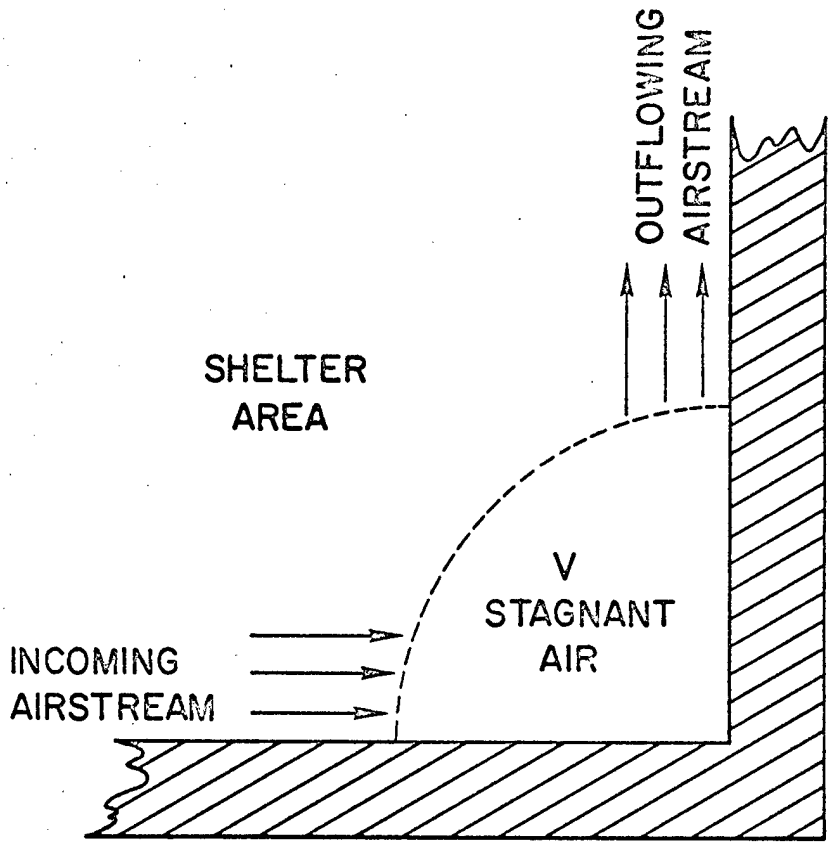

FIGURE E-9F DEFLECTION OF AIRSTREAM IN CORNER

and eventually flows out of the corner in a direction perpendicular to the direction of inflow. After inflow into the corner develops, there is a time delay during which static pressure builds up throughout an increasing volume of stagnant air V. This increasing static pressure drives the outflow in ever-increasing magnitude. If inflow remains steady, presumably an equilibrium is achieved such that inflowing mass matches the mass flowing out.

If temperature equilibrium is also reached, then kinetic energy of inflow must equal the energy of outflow. Thus, the net result after enough time has passed is a pure deflection of the incoming stream. In small shelters subjected to megaton nuclear weapon effects, this is the condition to be expected.

Behavior of an airstream in the corner illustrated in Figure E-9F differs from that suggested by Figure E-9D in that the areas A_1 and A_2 need not be equal, and temperature equilibrium between the holding room and shelter space need not be reached while blast pressures against the structure exist.

III. Multiple Rooms

Although the algebra becomes increasingly cumbersome as rooms are added, the foregoing principles of calculation can be applied to a series of connected rooms. For example, two rooms are represented in Figure E-11 for which two control surfaces may be employed. Through the smaller the momentum flux is due to flow through the first doorway and the resulting momentum equation may be written as:

$$A_2 (P_1 - P_2) = \rho_2 u_2^2 A_2 \qquad (32)$$

Using the larger control surface we find:

$$(P_1 - P_3') A_2 + (P_3' - P_4) A_4 = \rho_4 u_4^2 A_4 \tag{33}$$

Method G employs the two equalities below during filling:

$$P_2 = P_3' \tag{34}$$

$$P_4 = P_5' \tag{35}$$

Equations governing flow into the first of the two connected rooms can be written as follows:

$$\frac{\gamma}{\gamma-1} \cdot \frac{P_1}{\rho_1} = \frac{\gamma}{\gamma-1} \cdot \frac{P_2}{\rho_2} + \frac{1}{2} u_2^2 \tag{36}$$

$$\rho_2 = \rho_1 \left(\frac{P_2}{P_1}\right)^{\frac{1}{\gamma}} \tag{37}$$

To these two equations one of the two possible pressure relations represented by Eqs. (32), or (34) must be added to form a complete system from which P_2, u_2, and ρ_2 for the time interval under consideration may be calculated.

Under Methods F and G, the equations governing flow into the first of two rooms are identical to those from which the filling of a single room is computed. Calculation of flow into the second or inner room is more complicated however.

Because observed pressure buildup in two connected rooms has not generally followed simple calculations based on an assumption of uniform pressures over the control surfaces of Figure E-10, provision will be made in the analysis at the outset for a correction term Δ. The quantity Δ will be chosen to reconcile momentum balances based on inner and outer control surfaces such as those shown in Figures E-3 and E-7, that is,

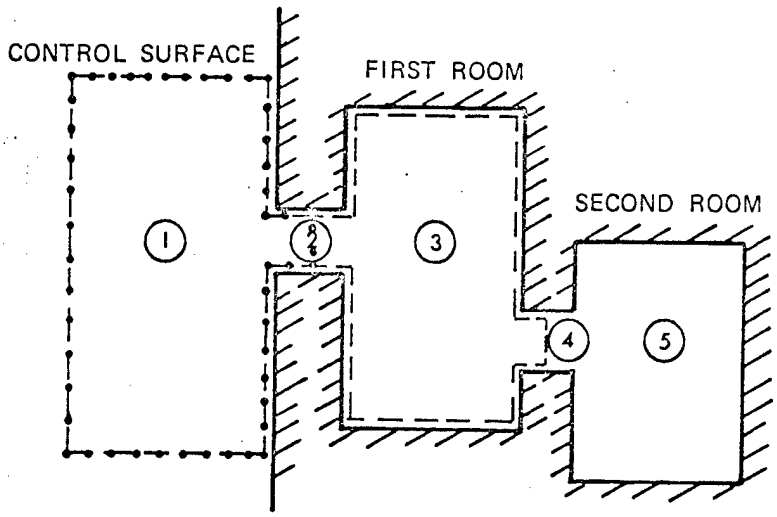

FIGURE E-10 CONTROL SURFACE USED IN CALCULATING FLOW INTO SECOND ROOM

$$(P_3' - P_2)\ A_2 + \Delta = (P_1 - P_2)\ A_2$$

or,

$$\Delta = (P_1 - P_3')\ A_2 \tag{38}$$

Generalizing, we will take the correction terms, Δ, equal to the pressure differential across the duct times the area of the duct. Thus, the corrected Eq. (33) becomes:

$$(P_3' - P_4)\ A_4 = \rho_4\ u_4^2\ A_4 \tag{39}$$

During filling of the second room, there will be an average wind moving through the first room into the second doorway. If u_3 is the speed of this wind and A_3 is the cross sectional area of the first room, then, in view of the quasi-steady state assumption, conservation of energy implies

$$\frac{\gamma}{\gamma-1} \cdot \frac{P_3'}{\rho_3'} + \frac{1}{2}\ u_3^2 = \frac{\gamma}{\gamma-1} \cdot \frac{P_4}{\rho_4} + \frac{1}{2}\ u_4^2 \tag{40}$$

and conservation of mass implies

$$\rho_3\ u_3\ A_3 = \rho_4\ u_4\ A_4 \tag{41}$$

and the assumption of isentropy leads to

$$\rho_4 = \rho_3' \left(\frac{P_4}{P_3'} \right)^{\frac{1}{\gamma}} \tag{42}$$

Eqs. (39), (40), (41), and (42) make it possible to compute by Method F the four unknowns:

$$\rho_4,\ u_4,\ P_4 \text{ and } u_3$$

The resulting solution for P_4 can be put in a form similar to that used in computing P_2

$$\frac{2\gamma}{\gamma+1}\left(\frac{P_4}{P'_3}\right)^{1/\gamma} = \frac{P_4}{P'_3} + \frac{\gamma-1}{\gamma+1}\left[1-\left(\frac{A_4}{A_3}\right)^2\left(\frac{P_4}{P'_3}\right)^{2/\gamma}\right]$$

$$+\frac{\gamma-1}{\gamma+1}\left[\frac{A_4}{A_3}\left(\frac{P_4}{P'_3}\right)^{1/\gamma}\right]^2 \frac{P_4}{P'_3} \qquad (43)$$

If $y = \dfrac{P_4}{P'_3}$

$$A = \frac{\gamma-1}{\gamma+1}\left\{\left[1-\left(\frac{A_4}{A_3}\right)^2\left(\frac{P_4}{P'_3}\right)^{2/\gamma}\right]+\left[\frac{A_4}{A_3}\left(\frac{P_4}{P'_3}\right)^{1/\gamma}\right]^2 \frac{P_4}{P'_3}\right\}$$

and $B = \dfrac{2\gamma}{\gamma+1}$

then Eq. (43) can be written as

$$B\, y^{1/\gamma} = y + A \qquad (44)$$

where in general $A = A(y)$; however, since $P_4 \leq P'_3$ and usually $A_4 \ll A_3$, the dependence of A on y is weak; i.e.:

$$A \cong \frac{\gamma-1}{\gamma+1} \qquad (45)$$

Use of Eq. (45) is equivalent to neglecting the average wind speed in the first room in Eq. (40).

After the duct parameters, i.e., ρ_2, P_2, u_2, ρ_4, u_4, and, if desired, u_3, have been found from the foregoing equations, then the new room pressures P_3 and P_5 and densities ρ_3 and ρ_5 are calculated:

$$\Delta m_5 \left(\frac{\gamma}{\gamma-1} \cdot \frac{P'_3}{\rho'_3} + \frac{1}{2} u_3^2 \right) = \frac{1}{\gamma-1} (P_5 - P'_5) V_5 \qquad (46)$$

where $\Delta m_5 = u_4 \rho_4 A_4 \Delta t$, mass increment in second room

$$\frac{\gamma}{\gamma-1} \cdot \frac{P_1}{\rho_1} \cdot \Delta m = \frac{1}{\gamma-1} (P_3 - P'_3) V_3 + \frac{1}{\gamma-1} (P_5 - P'_5) V_5 \qquad (47)$$

where $\Delta m = u_2 \rho_2 A_2 \Delta t$, mass increment in first room

$$\rho_5 = \rho'_5 + \frac{\Delta m_5}{V_5} \qquad (48)$$

$$\rho_3 = \rho'_3 + \frac{\Delta m - \Delta m_5}{V_3} \qquad (49)$$

Outflow from both the first and second rooms is treated with similar basic equations except Eq. (37) is replaced by

$$\rho_2 = \rho'_3 \left(\frac{P_2}{P'_3} \right)^{1/\gamma} \qquad (50)$$

and Eq. (42) by

$$\rho_4 = \rho'_5 \left(\frac{P_4}{P'_5} \right)^{1/\gamma} \qquad (51)$$

Again, in the computation of outflow parameters in the first doorway (i.e., ρ_2, P_2 and u_2) Eqs. (32), (36), and (37) are used as set forth above when only a single room was considered. For outflow through the second doorway, two cases should be distinguished: (1) there is inflow through the first doorway and (2) flow through the first doorway is outward. These conditions affect the form of Eqs. (33) and (40). In case (1), $u_3 = 0$, and Eq. (40) simplifies to:

$$\frac{\gamma}{\gamma-1} \cdot \frac{P'_3}{\rho'_3} = \frac{\gamma}{\gamma-1} \cdot \frac{P_4}{\rho_4} + \frac{1}{2} u_4^2 \qquad (52)$$

but Eq. (33) must contain two correction terms, Δ_3 and Δ_5, to account for excess force against the righthand and lefthand walls, respectively, of the first room:

$$(P_1 - P_3') A_2 - \Delta_3 + (P_3' - P_4) A_4 + \Delta_5 = \rho_4 u_4^2 A_4 \qquad (53)$$

where $\Delta_3 = (P_1 - P_3') A_2$ and $\Delta_5 = (P_5' - P_3') A_4$. Thus Eq. (53) becomes:

$$P_5' - P_4 = \rho_4 u_4^2 \qquad (54)$$

Combining Eqs. (51), (52), and (53), we find:

$$By^{1/\gamma} = y + A$$

where

$$y = \frac{P_4}{P_5'} \qquad (55)$$

$$B = \frac{2\gamma}{\gamma+1} \cdot \frac{\rho_5'}{\rho_3'} \cdot \frac{\rho_3'}{\rho_5'} \qquad (56)$$

$$A = \frac{\gamma-1}{\gamma+1} \left[\frac{P_3' + \Delta_5}{P_5'} \right] = \frac{\gamma-1}{\gamma+1} \qquad (57)$$

In case (2), there is net flow through the first room (i.e., $u_3 \neq 0$) Eq. (40) is unchanged but the analog of Eq. (33) is:

$$(P_1 - P_3') A_2 + (P_3' - P_4) A_4 + \Delta_5' = \rho_4 u_4^2 A_4 \qquad (58)$$

where

$$\Delta_5' = (P_5' - P_3') A_4 - (P_1 - P_3') A_2 \qquad (59)$$

This value of Δ_5' is computed by equating the force tending to drive the air out of the second room, i.e., $(P_5' - P_4) A_4$

to the momentum flux stopped in the first room and the outside reservoir, i.e.:

$$(P_1 - P_3') A_2 + (P_3' - P_4) A_4 + \Delta_5' .$$

Solving Eqs. (40), (41), (51), and (58), we find again that

$$By^{1/\gamma} = y + A$$

where x and B are given by Eqs. (55) and (56), but now

$$A = \frac{\gamma+1}{\gamma-1}\left\{(1-\alpha^2)\left[\frac{P_1 - P_3'}{P_5'}\cdot\frac{A_2}{A_4} + \frac{P_3' + \Delta_5'}{P_5'}\right] + \alpha^2 y\right\} \tag{60}$$

and

$$\alpha = \frac{A_4}{A_3}\cdot\frac{\rho_5'}{\rho_3'}\cdot y^{1/\gamma} \tag{61}$$

Substituting Eq. (59) into Eq. (61),

$$A = \frac{\gamma+1}{\gamma-1}\left\{(1-\alpha^2) + \alpha^2 y\right\} \tag{62}$$

Since, ordinarily, $A_3 \gg A_4$, and $y < 1$, $\alpha^2 \ll 1$, from which we conclude:

$$A \approx \frac{\gamma+1}{\gamma-1} \tag{63}$$

An alternative expression for A in case (2) can be found by writing the excess force on the wall against which the outflow from the second room is directed as the pressure differential across the duct times the duct area:

$$\Delta_5'' = (P_5' - P_3')\ A_4 \tag{64}$$

Substituting Δ_5'' from Eq. (64) for Δ_5' in Eq. (60), we compute for the constant term

$$A = \frac{\gamma+1}{\gamma-1}\left\{(1-\alpha^2)\left[\frac{P_1 - P_3'}{P_5'}\cdot\frac{A_2}{A_4} + 1\right] + \alpha^2 y\right\} \tag{65}$$

for which small α becomes

$$A = \frac{\gamma+1}{\gamma-1}\left[\frac{P_1 - P_3'}{P_5'}\cdot\frac{A_2}{A_4} + 1\right] \tag{66}$$

One final case remains to be considered, namely, outflow through the first doorway combined with inflow through the second. Conditions in the second doorway are computed by solving Eq. (40) with $u_3 = 0$, Eq. (42) and

$$(P_1 - P_3')\ A_2 + (P_3' - P_4)\ A_4 = \rho_4\ u_4^2\ A_4 \tag{67}$$

These equations lead to Eq. (44) in which

$$y = \frac{P_4}{P'_3}$$

$$B = \frac{2\gamma}{\gamma+1}$$

$$A = \frac{\gamma-1}{\gamma+1}\left[\left(\frac{P_1}{P'_3} - 1\right)\frac{A_2}{A_4} + 1\right]$$

In summary then we see that in every case an equation of the form $By^{1/\gamma} = y + A$ must be solved for y. This equation is encountered also in the first doorway if Method F is used. In Table E-2 the meanings of y, A, and B for each case are listed. Since conditions in the first doorway under Method F are independent of conditions inside, the definitions for the first duct appear separately.

In Figure E-11 results of a calculation carried out by Method F for two rooms are compared with measurement[23] of average pressure in the first room. The two rooms consisted of two small models such as those illustrated in Figures E-5 and E-6 placed back to back with a connecting door exactly like the outside door. The experiment was performed in a shock tube in which the wave struck the first doorway head-on. Also in Figure E-11 appears the result of a calculation treating the whole volume of the two model rooms as if it were in a single room. In Figure E-12 measured and calculated results for the second room in the model appear. At least in this one example, all three calculated pressure rises, i.e., in the first room, in the second room, and in the whole volume of both rooms treated as a single room, are quite similar and there appears to be no advantage in using the complicated procedures for computing the fill of two connected rooms.

The calculated histories shown in Figures 11 and 12 have not been carried beyond the time of equilibrium between inside and outside pressures.

Figure E-13 shows pressure history calculated by Method D ignoring the wall between rooms. For this calculation the discharge coefficient has been set equal to 0.7 on inflow and 1.0 for outflow.*

---

* CAVFIL, a FORTRAN program written at IIT Research Institute, was used to make the computation

Table E-2

MEANINGS OF y, A, AND B IN THE EQUATION $By^{1/\gamma} = y + A$ WHEN METHOD F IS USED

First doorway

Inflow

$$y = \frac{P_2}{P_1}$$

$$B = \frac{2\gamma}{\gamma + 1}$$

$$A = \frac{\gamma - 1}{\gamma + 1}$$

Outflow

$$y = \frac{P_2}{P_3'}$$

$$B = \frac{2\gamma}{\gamma + 1} \cdot \frac{\rho_3'}{\rho_1} \cdot \frac{P_1}{P_3'}$$

$$A = \frac{\gamma - 1}{\gamma + 1} \cdot \frac{P_1}{P_3'}$$

Second doorway

Inflow Both Doors

$$y = \frac{P_4}{P_3'}$$

$$B = \frac{2\gamma}{\gamma + 1}$$

$$A = \frac{\gamma - 1}{\gamma + 1} \left[1 - \left(\frac{A_4}{A_3} y^{1/\gamma} \right)^2 (1 - y) \right]$$

Table E-2 (concluded)

Outflow Both Doors

$$y = \frac{P_4}{P_5'}$$

$$B = \frac{2\gamma}{\gamma + 1} \cdot \frac{\rho_5'}{\rho_3'} \cdot \frac{P_3'}{P_5'}$$

$$A = \frac{\gamma + 1}{\gamma - 1} \left[1 - \alpha^2 (1 - y)\right]$$

$$\alpha = \frac{A_4}{A_3} \cdot \frac{\rho_5'}{\rho_3'} y^{1/\gamma}$$

or alternatively

$$A = \frac{\gamma + 1}{\gamma - 1} \left\{(1 - \alpha^2) \left[\frac{P_1 - P_3'}{P_5'} \cdot \frac{A_2}{A_4} + 1\right] + \alpha^2 y\right\}$$

Inflow First Door/Outflow Second Door

$$y = \frac{P_4}{P_5'}$$

$$B = \frac{2\gamma}{\gamma + 1} \cdot \frac{\rho_5'}{\rho_3'} \cdot \frac{P_3'}{P_5'}$$

$$A = \frac{\gamma - 1}{\gamma + 1}$$

Outflow First Door/Inflow Second Doorway

$$y = \frac{P_4}{P_3'}$$

$$B = \frac{2\gamma}{\gamma + 1}$$

$$A = \frac{\gamma - 1}{\gamma + 1} \left[\left(\frac{P_1}{P_3'} - 1\right) \frac{A_2}{A_4} + 1\right]$$

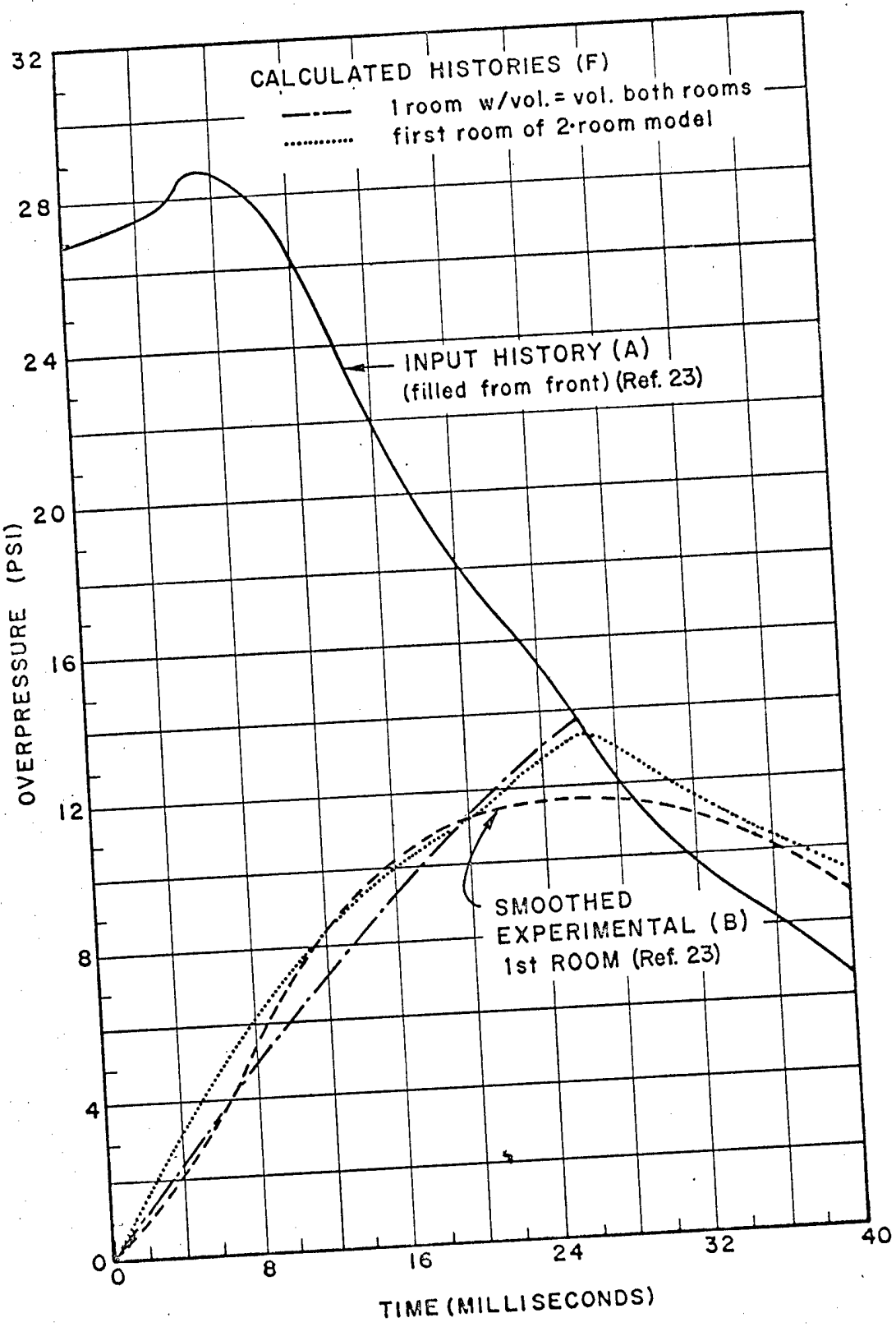

FIGURE F-11 COMPARISON OF OBSERVATIONS IN THE FIRST ROOM OF A TWO-ROOM MODEL WITH CALCULATIONS BY METHOD F

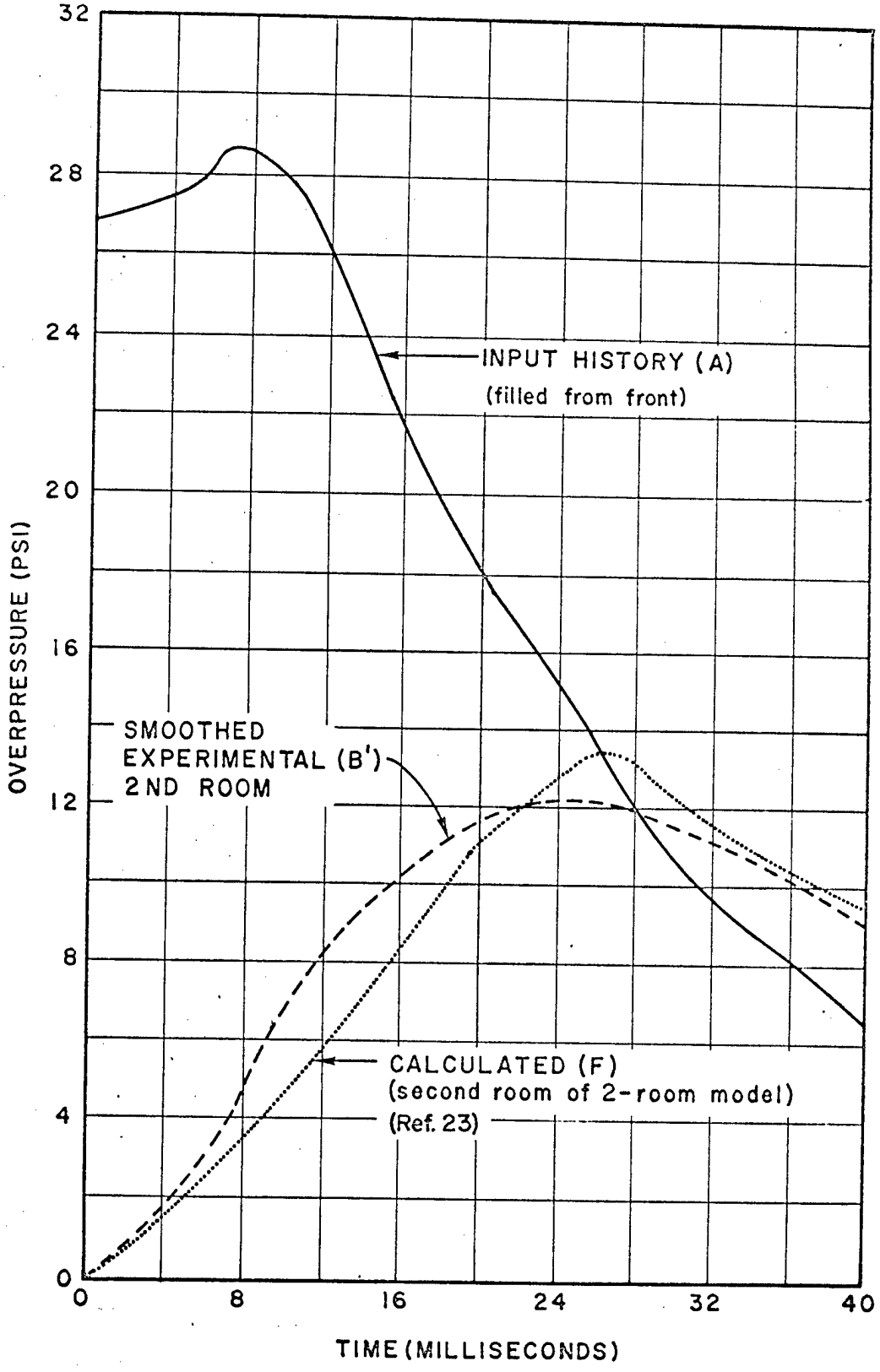

FIGURE E-12 COMPARISON OF OBSERVATIONS IN THE SECOND ROOM OF A TWO-ROOM MODEL WITH CALCULATIONS BY METHOD F

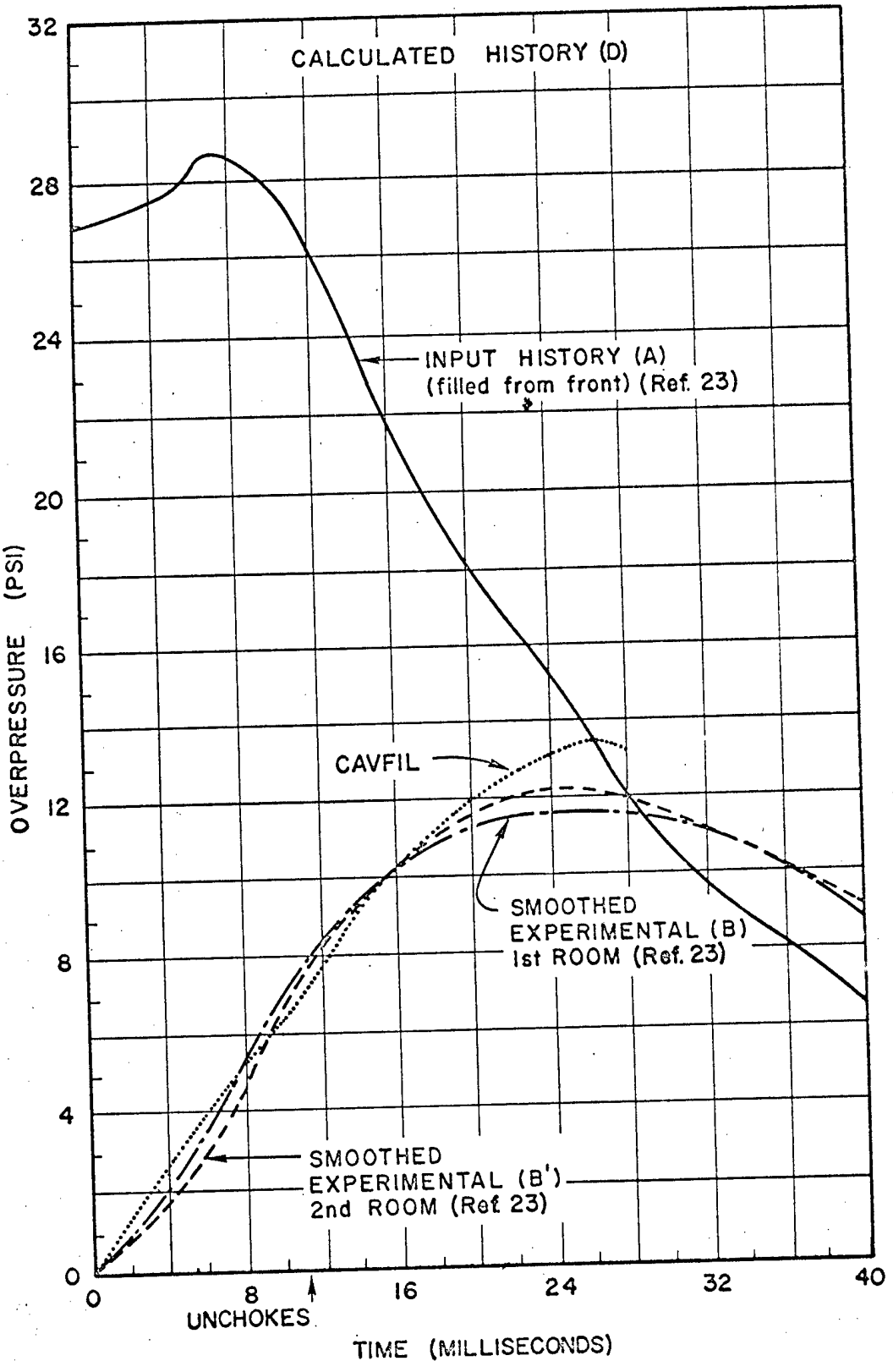

FIGURE E-13 COMPARISON OF OBSERVATIONS IN TWO-ROOM MODEL WITH CALCULATIONS BY METHOD D

The outside pressure, labeled "input history" in Figures E-11, E-12, and E-13, was measured as the stagnation pressure on the front face of the model simultaneously with the measurements of interior pressures. The short-lived reflected wave does not appear in these external histories.

IV Openings into Different Pressure Fields

The simple methods considered under the heading General Case in Section II above can easily be extended to the case of simultaneous flow into a single room through several openings, each of which is exposed to a separate outside pressure history. This situation will arise, for example, when a nuclear blast wave sweeps over a building, striking one of the four walls head-on, two side-on and exposing the fourth to the wake of the wave. The roof would be struck partially head-on if the explosion were an air burst, or side-on if the burst were on the ground. Head-on impact produces a strong but brief reflected wave followed by a quasi-steady wind and an associated strong drag force superimposed upon the static pressure. When impact is not head-on, only the drag and static pressures are ordinarily taken into account. References 1 and 3 contain discussions of methods of estimating outside pressure in these cases.

A. Computer Program

A computer program has been written in time-share FORTRAN to calculate average pressure as a function of time inside an open room exposed to a nuclear blast wave. Dynamic pressure in each opening may be obtained also. Characteristics of the room, the wave and ambient conditions are typed by the operator in response to typed questions. Provision is made for a maximum of eight openings and the delays between wave front arrival at the leading face of the building and each opening must be supplied. Only three different pressure histories, however, are available for assignment to each opening: the history associated with head-on impact, and two others which contain only the static pressure behind the front and a drag force. Three different drag coefficients must be specified, one for the history associated with head-on impact and one each for the two remaining histories. In order to relate each opening to one of the three possible histories a "location code" is specified for each opening. This code is the number 1 for the head-on history and the numbers 2 and 3 for the remaining two histories.

Duration of reflected pressure ("clearing time") against the wall struck head-on is not calculated in the program but must be entered by the operator. Other details of blast history are however calculated according to algorithms based on descriptions given in References 1 and 3.

The operator may choose certain features of the presentation of the program output. He may have outside (or "input") pressure histories at

each opening listed (pressures as functions of time); he may limit program output to peak room pressures (both static and dynamic) or he may choose to have only the history in the room during pressure build-up presented. Finally he must indicate whether or not he wants dynamic pressure histories in each opening presented.

By answering .TRUE. to the program question WANT TRANSLATION EFFECTS (.TRUE. OR .FALSE.)?, and supplying an acceleration coefficient when requested, the user may learn peak speeds achieved by bodies originally placed at grid points within the jet. This part of the program will also yield the coordinates of the points where these peak speeds are reached. (The coordinate system measures x-coordinate along a centerline through the opening, zero opposite the inner face of the opening, and y-coordinate perpendicular to the centerline.) In making these calculations, the program assumes that there are no obstacles of any kind in the path of these objects nor any friction associated with their motion.

It should be pointed out that the state of knowledge at this time does not justify great reliance upon all parts of the numerical solution to any given problem. Values of dynamic pressure in particular have not been compared with measurements. However, calculated values are conservative for purposes of damage assessment. Calculated values of room pressure during outflow through one or more openings probably do not accurately reflect the relatively small actual pressure differential between inside and outside.

The program algorithm is based on Method F. A partial value of Δm_3 is calculated for each opening corresponding to each time step Δt and inside pressure P_3'. The sum of the partial values for all openings becomes Δm. The equation

$$By^{1/\gamma} = y + A$$

is solved during outflow in a subroutine. When two solutions for $y < 1$ exist the larger is chosen.

A listing of the computer program appears in Table E-3.

B. Numerical Example

As an indication of how the foregoing general procedures may be modified to account for several openings a brief numerical example will be carried out here.

Consider a volume contained in two rooms connected to each other by an open doorway and consider each room connected to the outside by a single doorway, as shown in Figure E-14. The blast wave that sweeps ove the structure will be characterized by a free field overpressure of 10

Table E-3
COMPUTER PROGRAM

```
      C0MM0N G2,G3,L3,0(100,8),T(100),A(8,2),NWIN,NT,C
      L0GICAL L1,L2,L3,L4,L5,L6,L7
      DIMENSI0N P(100),N(8),02(8),P0UT(8)
      PRINT,"AMBIENT AIR PRESSURE (PSI)"
      INPUT,P0
      PRINT,"AMBIENT AIR DENSITY (LB/CF)"
      INPUT,RH00
      PRINT,"R00M V0LUME (CF)"
      INPUT,V3
      PRINT,"NUMBER 0F 0PENINGS (N0T M0RE THAN 8)"
      INPUT,NWIN
      PRINT,"AREAS 0F EACH 0PENING (SQFT)"
      INPUT,(A(I,1),I=1,NWIN)
      PRINT,"L0CATI0N C0DE F0R EACH 0PENING"
      INPUT,(N(I),I=1,NWIN)
      PRINT,"DELAY IN ENTRY AT EACH 0PENING (MSEC)"
      INPUT,(A(I,2),I=1,NWIN)
      PRINT,"CLEARING TIME (MSEC)"
      INPUT,TC
      PRINT,"DRAG C0EFFS: FR0NT, SIDE AND REAR"
      INPUT,CDFF,CDFS,CDFR
      PRINT,"PEAK FREE FIELD 0VERPRESSURE (PSI)"
      INPUT, PS0
      PRINT, "DURATI0N 0F P0SITIVE PHASE (SEC)"
      INPUT, T0
      TC=TC/1000.
      PRINT,"WANT PEAK VALUES 0NLY (.TRUE. 0R .FALSE.)"
      INPUT,L1
      IF(L1)G0 T0 3
      PRINT,"INTERVAL BETWEEN VALUES 0F 0UTPUT (MSEC)"
      INPUT,TI
      TI=TI/1000.
      PRINT,"WANT  DECLINE 0F R00M PRESSURE (.TRUE. 0R .FALSE.)"
      INPUT,L2
      G0 T0 5
    3 TI=T0/99.
      L2=.FALSE.
    5 L3=.FALSE.
      L7=.FALSE.
      PRINT,"WANT 0UTSIDE PRESSURE (.TRUE. 0R .FALSE.)"
      INPUT,L5
      IF(L5)PRINT 26
      PR=2.*PS0*(7.*P0+4.*PS0)/(7.*P0+PS0)
      PD0=2.5*PS0*PS0/(7.*P0+PS0)
      PSC=PS0*(1.-TC/T0)*EXP(-TC/T0)
      PDC=PD0*(1.-TC/T0)*(1.-TC/T0)*EXP(-2.*TC/T0)
      PC=PSC+PDC
      NT=T0/TI+1
      IF(NT.LE.100)G0 T0 13
      PRINT,"***VECT0R 0VERL0ADED - TIME INTERVAL TRUNCATED"
      NT=100
   13 G=1.4; G2=1./G ; G3=1.-G2 ; G4=2./G3
      G5=G+1.; G6=2.*G/G5; G7=(G-1.)/G5
      G9=.1912**G2
      GP0=2.*G*P0 ; GPS=2.*G*(PS0+P0)
      RH010=RH00*(GP0+G5*PS0)/(GP0+(G-1.)*PS0)
      RH011=RH010*(GPS+G5*(PR-PS0))/(GPS+(G-1.)*(PR-PS0))
      C=SQRT(G*P0*32.*144./RH00)
      D0 7 I=1,NWIN
      02(I)=0.
      A(I,2)=A(I,2)/1000.
    7 C0NTINUE
      P30=P0 ; RH030=RH00
      TT=0. ; T0=0.
      TAU=2.*(V3**(1./3.))/C
      DT=TAU/10.
      DDT=DT
    9 IF(TI-2.*DDT)10,11,11
   10 DDT=DDT/2.
      G0 T0 9
   11 IST0P=TI/DDT+1
      DDT=TI/IST0P
      MC=-1
      D0 990 J=1,NT
      IF(J.GT.100)G0 T0 992
      D0 99 I=1,IST0P
      MC=MC+1
      MD=2 ; II=I
      IF(MC.NE.0)G0 T0 62
      II=I-1 ; MD=1
   62 TT=T0+II*DDT
      IF(TT.GT.T0)G0 T0 99
      R=TT/T0 ; RR=1.-R
      PD=PD0*RR*RR*EXP(-2.*R)
      PS=PS0*RR*EXP(-R)
      DM=0. ; W=0.
      D0 500 K=1,NWIN
      M=N(K) ; DLY=A(K,2)
      IF(DLY.GT.TT)G0 T0 500
      PS1=PS0+P0
      RH012=RH010
      G0 T0 (15,16,17),M
   15 CDF=CDFF
      IF(TT-TC)20,20,21
   20 P11=(TC-TT)*(PR-PC)/TC+PC
      RH012=RH011
      PS1=PR+P0
      G0 T0 30
   16 CDF=CDFS
      G0 T0 21
   17 CDF=CDFR
   21 P11=PS+CDF*PD
   30 P0UT(K)=P11
      P11=P11+P0
```

```
      RH01=RH012*((P11/PS1)**G2)
      IF(P11-P30)36,35,37
 35   U22=0.
      GO TO 39
 36   JSIGN=-1
      AA=G7*P11/P30
      BB=G6*RH030*P11/(RH01*P30)
      Z=P11/(RH01**G)
      Y=.9094*P30/(RH030**G)
      IF(Y.GT.Z)GO TO 60
      CALL EQ(AA,BB,P2)
      IF(.NOT.L3)GO TO 303
      NT=J
      GO TO 19
 60   PRINT,"Y.GT.Z" ; GOTO 999
303   P2=P2*P30
      RH02=((P2/P30)**G2)*RH030
      X=P11/RH01
      GO TO 38
 37   JSIGN=+1
      P2=.1912*P11
      RH02=G9*RH01
      X=P11/RH01
 38   U22=G4*(X-P2/RH02)*32.*144.
      IF(U22)40,39,39
 40   PRINT,"U22 NEGATIVE",U22
      GO TO 999
 39   U2=SQRT(U22)*JSIGN
      Q2(K)=P11-P30
      GO TO (500,65),MD
 65   DDM=U2*RH02*A(K,1)*DDT
      DM=DM+DDM
      W=W+P11*DDM/(G3*RH01)
500   CONTINUE
      P3=P30*(G-1.)*W/V3
      RH03=RH030+DM/V3
      P3A=P30
      P30=P3 ; RH030=RH03
      IF(.NOT.L2 .AND. P3.LT.P3A)GO TO 80
      GO TO (19,99),MD
 80   L7=.TRUE.
      NT=J.
      GO TO 19
 99   CONTINUE
 19   T0=TT
      P(J)=P30-P0
      T(J)=TT
      IF(L5)PRINT 27,J,(POUT(K),K=1,NWIN)
      DO 18 L=1,NWIN
      Q(J,L)=Q2(L)
      Q2(L)=0.
 18   CONTINUE
      IF(L3)GO TO 992
      IF(L7)GOTO 800
990   CONTINUE
800   IF(L1)GOTO 991
      GO TO 992
991   PRINT 50,T(NT),P(NT),(Q(I,K),K=1,NWIN)
 50   FORMAT(1HO,30X,11HPEAK VALUES//1H 6HTIME= ,E11.4,1X,
     &3HSEC,4X,10HPRESSURE= ,E11.4,1X,4HPSIG//
     &18H DYNAMIC PRESSURES,1X,5H(PSI)/8(1H E11.4/))
      STOP
992   PRINT 22
      DO 993 I=1,NT
      PRINT 51,I,T(I),P(I)
993   CONTINUE
 22   FORMAT(1HO,15X,9HTIME(SEC),5X,14HPRESSURE(PSIG))
 51   FORMAT(1H ,I10,5X,E11.4,5X,E11.4)
      PRINT,"WANT TRANSLATION EFFECTS (.TRUE. OR .FALSE.)"
      INPUT, L6
      IF(L6)GOTO 995
      PRINT,"WANT VALUES OF DYNAMIC PRESSURE (TRUE OR FALSE)"
      INPUT,L4
      IF(.NOT.L4)GO TO 999
      PRINT 23
      DO 994 I=1,NT
      PRINT24,I,(Q(I,K),K=1,NWIN)
994   CONTINUE
      GOTO 999
995   CALL SLIDE
 23   FORMAT(1HO,15X,22HDYNAMIC PRESSURES(PSI)//)
 24   FORMAT(1H I10,3X,8(F5.2,2X))
 26   FORMAT(1HO,15X,23HOUTSIDE PRESSURES(PSIG)/)
 27   FORMAT(1H ,I10,3X,8(F6.2,1X))
999   STOP
      END
      SUBROUTINE EQ(A,B,X)
C SOLVES THE EQUATION B*(X**G2)=X+A FOR X
      COMMON G2,G3,L3
      LOGICAL L3
      X0=(B*G2)**(1./G3)
      F1=X0+A
      F2=B*(X0**G2)
      IF(F1-F2)1,2,3
 3    PRINT,"NO SOLN IN EQ"
      L3=.TRUE.
      RETURN
 2    IF(X0-1.)4,5,5
 5    PRINT,"NO SOLN IN EQ LT 1"
      L3=.TRUE. ; RETURN
 4    X=X0 ; RETURN
 1    N=0
      IF(X0-1.)8,42,7
 7    N=1
```


Table E-3 (continued)

```
2100    6  F1=1.+A
2110       IF(F1-B)9,10,11
2120    9  N=N+3 ; GØ TØ 12
2130   10  N=N+1 ; GØ TØ 12
2140   11  N=N+5
2150   12  GØ TØ (40,5,40,42,39,5),N
2160   39  XU=1. ; XL=XØ ; GØTØ 21
2170   40  XU=XØ ; XL=0. ; GØ TØ 21
2180   42  XU=1. ; XL=0. ; GØ TØ 21
2190   21  XM=(XU+XL)/2.
2200       R=(XU-XL)/XU
2210       IF(R-0.001)22,23,23
2220   23  F1=XM+A
2230       F2=B*(XM**G2)
2240       IF(F1-F2)24,22,25
2250   24  XU=XM
2260       GØ TØ 21
2270   25  XL=XM ; GØ TØ 21
2280   22  X=XM
2290   99  RETURN
2300       END
2310   SUBROUTINE SLIDE
2320   CØMMØN G2,G3,L3
2330   CØMMØN Q3(100,8),T(100),A(8,2),NWIN,NT,C
2340   PRINT,"ENTER ACCELERATIØN CØEFFICIENT (SØFT/LB)"
2350   INPUT,AA
2360   AA=AA*32.*144.
2370   PRINT 4
2380   4  FØRMAT(1ØH TIME(SEC),5X,28HCØRE DYNAMIC PRESSURES (PSI) )
2390   NT1=NT+1
2400   DØ 2 I=1,NT1
2410   2  PRINT 3,T(I),(Q3(I,J),J=1,NWIN)
2420   3  FØRMAT(1H F7.3,2X,8(F7.2,2X))
2430   DT=T(NT)/NT
2440   DØ 900 I=1,NWIN
2450   PRINT 7
2460   PRINT 5,I
2470   5  FØRMAT(13H ØPENING NØ. ,I1////16H INITIAL CØØRDS.,5X,
2480  & 13HFINAL CØØRDS.,5X,11HFINAL SPEED/16H  X (FT)  Y (FT),5X,
2490  &  16H  X (FT)  Y (FT),8X,5H(FPS)//)
2500   7  FØRMAT(1H //////)
2510   BØ=2.*SQRT(A(I,1)/3.14158)
2520   X1=4.5*BØ
2530   X2=X1+2.2*BØ
2540   X3=5.*X2
2550   DELX=X1/10.
2555   DELY=X1/2.
2560   NJ=INT(X3/DELX)+1
2565   NK=INT(X3/DELY)+1
2570   XØ=0.
2580   DLY=9.*BØ/C
2590   DØ 895 J=1,NK
2600   XØ=(J-1)*DELY
2610   PRINT," "
2620   Y=0.
2630   M=0
2640   DØ 890 K=1,NJ
2650   Y=(K-1)*DELX
2660   X=XØ
2670   V=0.
2680   DØ 880 L=1,NT
2690   IF(T(L).LT.DLY)GØTØ 200
2700   QØ=Q3(L,I)
2702   IF(QØ)15,18,18
2704   15  QØ=0.
2710   18  IF(X.GE.X1)GØTØ 50
2720   IF(Y.GT.(.1577*X+BØ/2.))GØTØ 20
2730   IF(Y.GT.BØ/2.)GØTØ 30
2740   GØTØ 40
2750   20  Q=0.
2760   M=1
2770   GØTØ 100
2780   30  B=.27*X
2790   E=(B-(Y-(X1-X)/9.))/B
2800   Q=QØ*(1.-(1.-E**1.5)**2.)**2.
2810   GØTØ 100
2820   40  R=Y/(X1-X)
2830   IF(R-.1111)42,42,30
2840   42  Q=QØ
2850   GØTØ 100
2860   50  IF(X-X2)60,60,70
2870   60  B=.27*X1+(.22*X2-.27*X1)*(X-X1)/(X2-X1)
2880   62  E=Y/B
2890   IF(E.GT.1)GØTØ 20
2900   Q=QØ*((1.-E**1.5)**4.)*((6.2*BØ/X)**2.)
2910   GØTØ 100
2920   70  B=.22*X
2930   GØTØ 62
2940   100  V=V+AA*Q*DT
2950   X=X+V*DT
2960   IF(M-1)880,220,220
2970   200  QØ=Q3(L,I)*T(L)/DLY
2980   GØTØ 18
2990   220  PRINT 25,XØ,Y,X,Y,V
3000   GØTØ 895
3010   880  CØNTINUE
3020   PRINT 25,XØ,Y,X,Y,V
3030   25  FØRMAT(1H ,F6.1,2X,F6.1,6X,F6.1,2X,F6.1,8X,F6.1/)
3040   890  CØNTINUE
3050   895  CØNTINUE
3060   900  CØNTINUE
3070   RETURN
3080   END
```

Table E-3 (concluded)

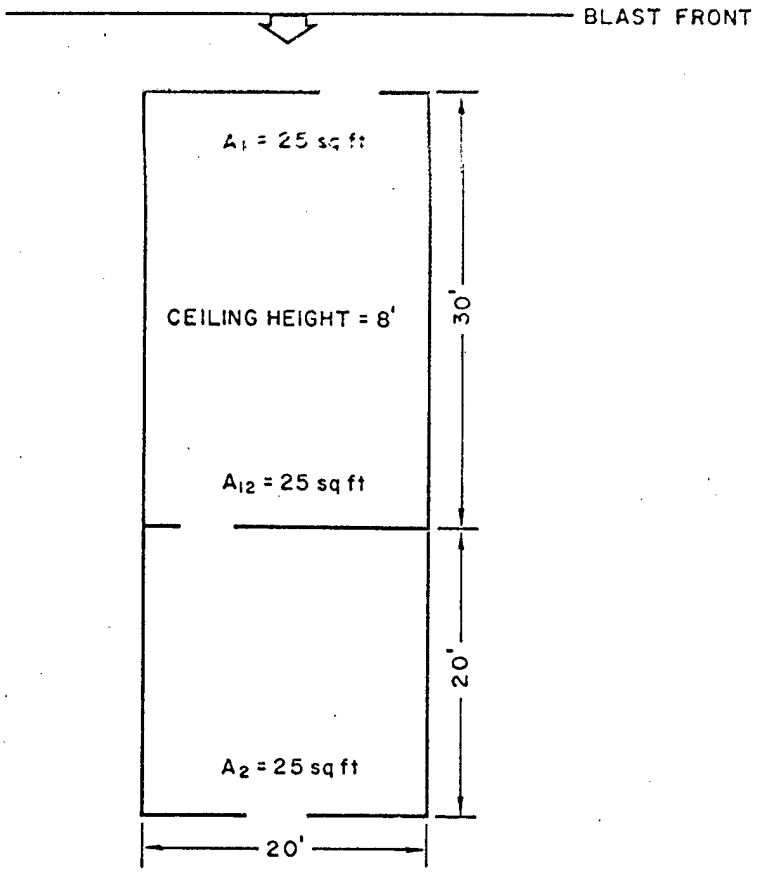

FIGURE E-14 SKETCH ILLUSTRATING NUMERICAL EXAMPLE

head-on incidence upon the opening to the larger room, and positive phase duration of 1 sec. Standard ambient conditions will be assumed, i.e., P_o = 14.7 psia and ρ_o = 0.0761 lb/ft^3. In the front wall the opening area is 25 ft^2 and there is a like opening in the rear wall. Because the door between the rooms has an area comparable to the area of each of the outside doors, the presence of the partition will be ignored and the volume to be filled taken as

$$V_3 = 50 \times 20 \times 8 = 8000 \text{ ft}^3$$

As a first step the pressure histories outside the two doors will be calculated, according to the procedures recommended by Ref. 1. Since the first window is struck head-on, there will be no time delay there and the peak pressure will be the reflected pressure P_R which is calculated as:

$$P_R = 2 \quad P_{so} \cdot \frac{7 P_o + 4 P_{so}}{7 P_o + P_{so}}$$

Here

P_{so} = 10 psi and P_o = 14.7 psi, hence

P_R = 25.3 psi

This reflected pressure will be felt in declining strength for the duration of the clearing time, t_c, which is estimated as

$$t_c = \frac{3s}{c}$$

where s is a dimension of the wall undergoing pressure clearing and c is sound speed. In this case

$$c = [\gamma P_o/\rho_o]^{1/2} = [1.4 \times 14.7 \times 32 \times 144/0.076096]^{1/2} = 1116 \text{ ft/sec}$$

and s = 20

so that

t_c = 53.7 ms

As an approximation the decline of reflected pressure during the interval

$$0 \leq t \leq t_c$$

is treated as linear, that is, at $t = t_c$ the pressure P_c on the first wall is simply the sum of the free field overpressure P_{sc} and the drag P_{dc} arising from the winds behind the shock front. Since during the time t_c free field pressure has fallen exponentially[1] from P_{so} = 10 psi

$$P_{sc} = P_{so} \left(1 - \frac{t_c}{t_o}\right) e^{-t_c/t_o}$$

where t_o is the free field duration of positive overpressure; in this case t_o = 1 sec so that

$$P_{sc} = 8.97 \text{ psi}$$

Peak drag pressure P_{do} is computed from the formula

$$P_{do} = \frac{5}{2} \cdot \frac{\left(P_{so}\right)^2}{7\,P_o + P_{so}} = \frac{5}{2} \cdot \frac{100}{7 \times 14.7 + 10} = 2.21 \text{ psi}$$

so that drag pressure at $t = t_c$ is:[1]

$$P_{dc} = P_{do}\left(1 - \frac{t_c}{t_o}\right)^2 \quad e^{\left(-2\ t_c/t_o\right)}$$

Numerically this is

$$P_{dc} = 1.78 \text{ psi}$$

Therefore the pressure outside the first opening at $t = t_c$ is:

$$P_c = P_{sc} + P_{dc} = 8.97 + 1.78 = 10.75$$

and, assuming a linear fall from P_{so} to P_c, for $0 \le t \le t_c$, pressure P_1 outside first wall as a function of time becomes:

$$P_1 = P_c + \frac{\left(t_c - t\right)}{t_c} \quad \left(P_R - P_c\right) \tag{68}$$

For the remainder of the positive phase duration outside pressure at the first opening is simply the sum of the decayed side-on pressure

$$P_s = P_{so} \quad \left(1 - \frac{t}{t_o}\right) e^{-t/t_o} \tag{69}$$

and decayed dynamic pressure

$$P_d = P_{do} \left(1 - \frac{t}{t_o}\right)^2 e^{-2t/t_o} \qquad (70)$$

so that for $t_o > t > t_c$

$$P_1 = P_s + P_d \qquad (71)$$

For the first wall a drag coefficient equal to + 1.0 has been tacitly assumed above but for the second opening this coefficient will be different from 1, and according to Ref. 1, a value of -0.4 may be assumed. At the rear opening there is no reflected pressure and the delay is equal to the time taken by the front to traverse the building (assuming that the opening is already open upon blast arrival or that it is immediately forced open by the blast). Blast front speed can be found from the formula[1]

$$U = c_o \left[1 + \frac{\gamma + 1}{2} \cdot \frac{P_{so} - P_o}{P_o}\right]^{1/2}$$

where c_o = sound speed in ambient air, i.e.,

$$c_o = \left[\gamma P_o \, 32 \times 144/\rho_o\right]^{1/2} = 1116 \text{ ft/sec}$$

Hence

$$U = 1116 \times \left[1 + \frac{2.4}{2.8} \times \frac{10}{14.7}\right]^{1/2} = 1148 \text{ ft/sec}$$

so that delay at the rear entrance is $\frac{50}{1148} = 43.5$ ms

Beginning at t = 43.5 ms the room starts to fill through the rear opening. (Outflow through openings other than the first can ordinarily be neglected during the delay period: either the other openings are closed to the blast for a certain period or, if not, the blast travel time to them is much shorter than the time required to start outflow through them.) Filling through the rear opening takes place however from a reservoir at lower pressure than that outside the front opening, i.e., outside pressure P_{1r} at the rear is:

$$P_{1r} = P_s - 0.4 P_d \qquad (72)$$

The decline in P_{so} and P_{do} which occurs while the blast front travels from front to rear opening is negligibly small and may be safely neglected for buildings of ordinary size.

For this sample case, the quantities P_1 (pressure outside the front opening) and P_{1r} (pressure outside the rear opening) have been calculated as functions of time and plotted in Figure E-15. The figure shows the discontinuity in the derivative of P_1 with respect to time at the point (t_c, P_c) when the reflected pressure is assumed to disappear and the outside pressure takes on its quasi-steady value.

Also plotted in the figure are inside pressure histories P_3 calculated by two methods: the greatly simplified procedure given in section II-A of this report and the step-by-step method F explained in Section II-B. According to the first of these two procedures the estimated history is given by the line segments ODFG obtained as follows. When the blast arrives at the front opening, filling immediately begins along line OA, where point A is the intersection of the outside pressure history and the abscissa

$$t = \frac{V_3}{2A_1} = \frac{8000}{2 \times 25} = 160 \text{ ms}$$

Line BC is a similar line representing filling through the rear opening, beginning after the delay time of 43.5 ms. Ordinates under the line BC have been added to ordinates of OA to produce the line DE. Since areas of both openings are equal, the point F is placed halfway between current outside pressures outside the front and rear openings and the decline of P_3 represented schematically by the line FG.

The step-by-step calculation results in the curve labelled "Method F" in Figure 15. Because of the high reflected pressure during the interval $0 \leq t \leq t_c$ (which does not influence the results of the simplified method in this example) the more careful calculation shows a faster build-up of room pressure than the line ODF. To demonstrate the method the first step of the stepwise solution will be calculated below.

Since the least sound transit time across the room is approximately 20 ms we will choose a value of $\Delta t = 5$ ms. At $t = 0$ there is only one opening, that in the front wall. Outside pressure there at that time is $P_R = 25.3$ psig. Inside pressure $P_3' = P_o = 14.7$ psia and density is $\rho_3' = \rho_o = 0.076096$ lb/ft^3.

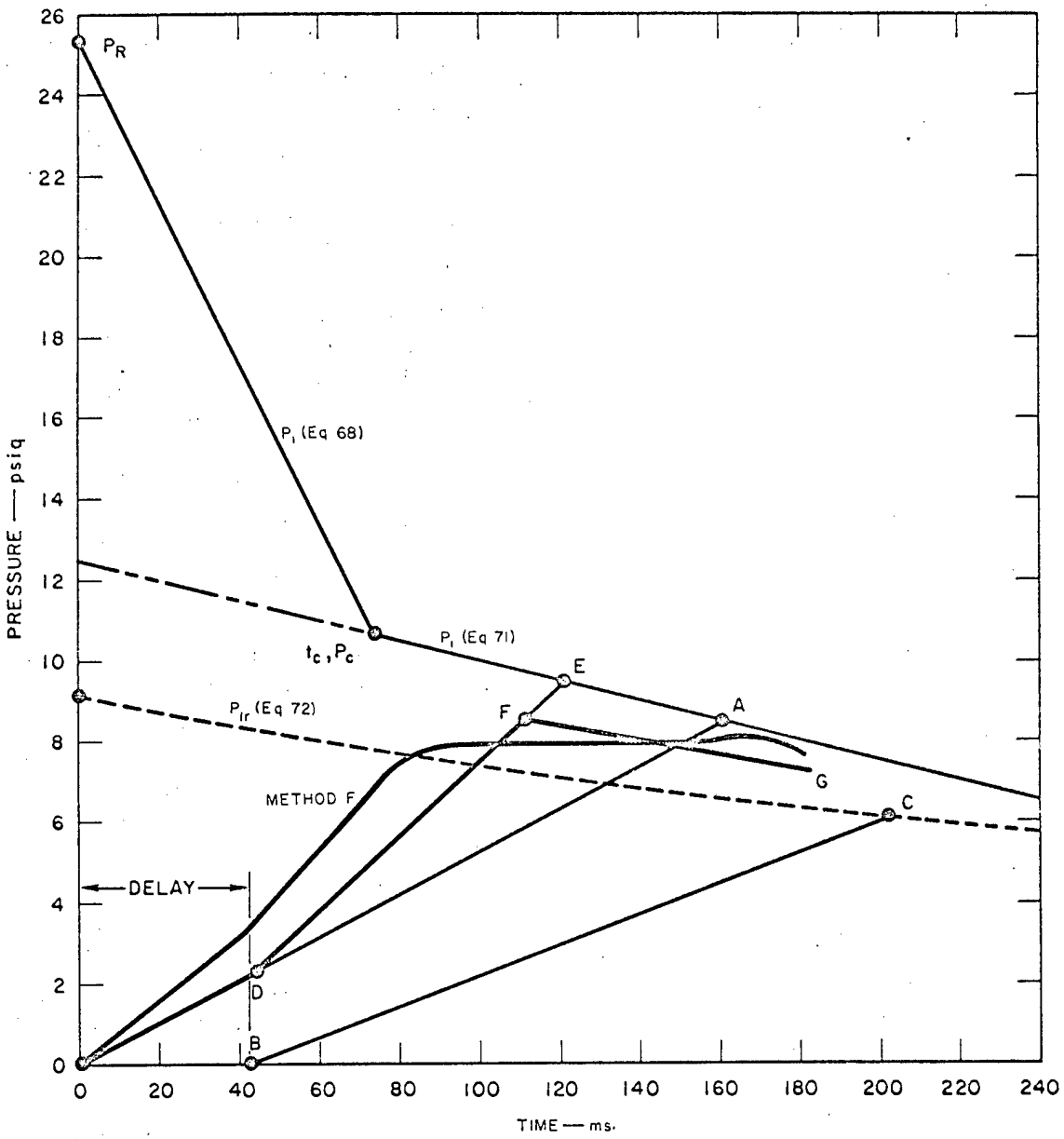

FIGURE E-15 ILLUSTRATIVE EXAMPLE

1. $P_1 = 25.3 + 14.7 = 40.0$ psia

2. $\rho_1 = \left[\frac{P_1}{P_0}\right]^{1/\gamma} \quad \rho_o = \left[\frac{40.0}{14.7}\right]^{1/1.4} (0.076096) = 0.156 \text{ lb/ft}^3$

3. $P_2 = 0.1912 \quad P_1 = (0.1912) \quad (40.0) = 7.65$ psia

4. $\rho_2 = \left[\frac{P_2}{P_1}\right]^{1/\gamma} \quad \rho_1 = (0.307) \cdot (0.156) = 0.04785 \text{ lb/ft}^3$

5. $u_2^2 = \frac{2\gamma}{\gamma - 1}\left[\frac{P_1}{\rho_1} - \frac{P_2}{\rho_2}\right] = \frac{2.8}{0.4}\left[\frac{40.0}{0.156} - \frac{7.65}{0.04785}\right] 32 \times 144 = 3.11 \times 10^6 \frac{\text{ft}^2}{\text{sec}^2}$

6. $q_{21} = \frac{1}{2} \quad u_2^2 \quad \rho_2 = 7.45 \times 10^4 \frac{\text{lb/ft}}{\text{sec}^2}$ (dynamic pressure at front opening)

7. Since $P_1 > P_3'$: $u_2 > 0$, i.e., flow is inward. Were $P_3' > P_1$, u_2 would be negative

8. $\Delta m_{31} = u_2 \quad \rho_2 \quad A_2 \quad \Delta t = 0.0105$ lb

9. $\Delta w_{31} = \frac{P_1 \quad \Delta m_{31}}{\left(\frac{\gamma - 1}{\gamma}\right) \rho_1} = \frac{(40.0)(0.0105)}{\frac{0.4}{1.4} \quad (0.156)} \cdot 144 = 1360$ ft lb

10. Since the rear opening is closed at this time:

$$\Delta m_{32} = \Delta w_{32} = 0$$

Were the second opening available, steps 1 - 9 would be repeated using initial outside pressure at rear opening to calculate Δm_{32} and Δw_{32}

11. $\Delta m_3 = \Delta m_{31} + \Delta m_{32} = 0.0105$ lb

12. $\Delta w_3 = \Delta w_{31} + \Delta w_{32} = 1360$ ft lb

13. $P_3 = P_3' + \frac{(\gamma - 1)\quad \Delta w_3}{V_3} = 14.7 + \frac{(0.4)(1360)}{8000} = 14.768$ psia (room pressure)

14. $\rho_3 = \rho_3' + \frac{\Delta m_3}{V_3} = 0.076096 + \frac{0.0105}{8000} = 0.0760973$ lb/ft^3 (air density in room)

15. Set P_3' equal to P_3 and ρ_3' equal to ρ_3 and return to step 1 with value of P_1 at $t = \Delta t = 5$ ms.

V. Edge Diffraction of an Acoustic Wave

A weak planar shock striking a semi-infinite wall head-on can be treated approximately as a self-similar acoustic wave in the manner demonstrated by Ludloff.[16] Such treatment is two-dimensional and neglects the presence of floor and ceiling.

In the acoustic approximation all disturbances or effects are propagated with sound speed. Thus after the incoming wave front strikes the semi-infinite wall, the influence of the edge will be felt only within a cylinder whose axis is the edge and whose radius is

$$c\,t$$

where c is sound speed and t is elapsed time after initial impact.

If a cartesian coordinate system is placed so that the edge becomes the z-axis and the negative y-axis lies in the wall the location of the circle of disturbance due to the wall is

$$x^2 + y^2 = c^2 t^2$$

and the equation satisfied by the overpressure p is

$$\frac{\partial^2 p}{\partial x^2} + \frac{\partial^2 p}{\partial y^2} = \frac{1}{c^2}\frac{\partial^2 p}{\partial t^2} \qquad (73)$$

If a change of variables is made:

$$\eta = \frac{y}{ct}, \quad \sigma = \frac{x}{ct}, \quad \text{and} \quad \tan\theta = \frac{y}{x} = \frac{\eta}{\sigma} \tag{74}$$

then in the new coordinates (η, σ, θ) the disturbance is confined to a circle of unit radius. If, further, radii are changed in scale according to the formula:

$$\rho = \frac{r}{1 + (1 - r^2)^{1/2}} \tag{75}$$

where ρ is the new radius and $r^2 = \eta^2 + \sigma^2$, then the equation satisfied by p in the cylindrical polar coordinates (ρ, θ) can be written

$$\rho \frac{\partial}{\partial \rho}\left(\rho \frac{\partial p}{\partial \rho}\right) + \frac{\partial^2 p}{\partial \theta^2} = 0 \tag{76}$$

This is Laplace's equation and is satisfied by the imaginary component of any analytic function of the complex variable.

$$\zeta = \rho\, e^{i\theta}$$

In the case of edge diffraction of a weak shock the present method yields a solution for $0 \le r \le 1$ (or $0 \le \rho \le 1$). The angle θ lies in the range $-\frac{\pi}{2}$ to $\frac{3\pi}{2}$, as illustrated in Figure E-16. The origin of coordinates is labelled O.

The boundary conditions are determined by physical considerations. Because the acoustic Eq. (73) or (76) is linear in p, the incident overpressure may be taken as unity and the pressure reflected from the wall, as 2. The overpressure in the undisturbed air is of course zero. These conditions imply the following pressure values on the circumference of the circle of disturbance

$$\left.\begin{aligned} -\frac{\pi}{2} \le \theta \le 0 \qquad & p = 0 \\ 0 \le \theta \le \pi \qquad & p = 1 \\ \pi \le \theta \le \frac{3\pi}{2} \qquad & p = 2 \end{aligned}\right\} \tag{77}$$

The areas of uniform pressure are marked in Figure E-16.

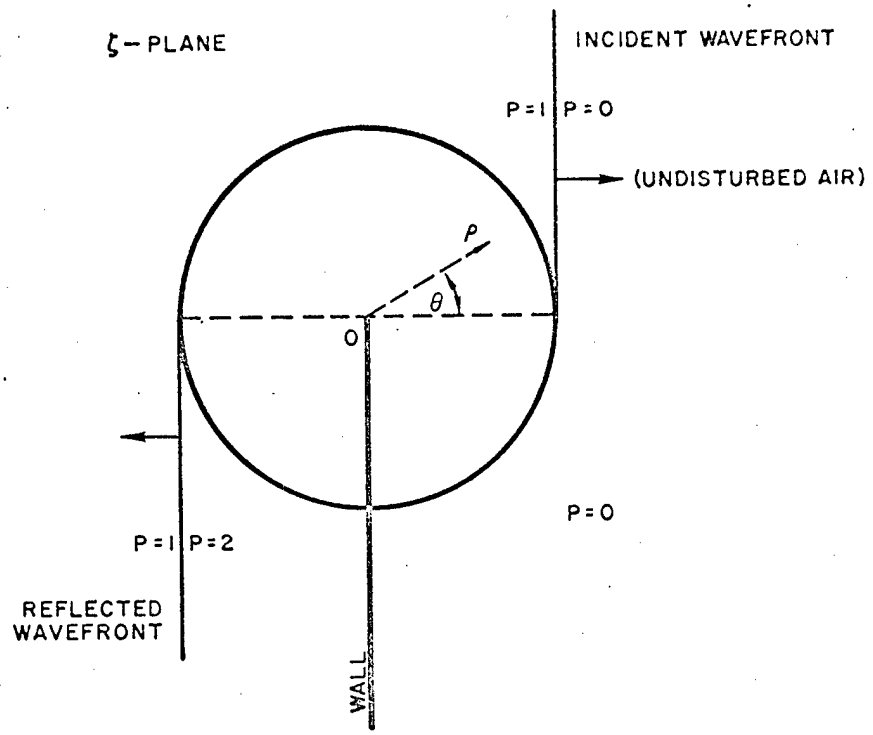

FIGURE E-16 BOUNDARY CONDITIONS ON CIRCLE OF INFLUENCE

Potential theory guarantees that there is only one pressure distribution within the unit circle which satisfies Eq. (76) and meets the foregoing boundary conditions. Solution of Eq. (76) will be guaranteed by the fact that the distribution function is analytic.

A further transformation of variable will make the exposition of the correct distribution function clear. Let

$$w = (i\zeta)^{1/2} = Re^{i\Phi} \tag{78}$$

where $R = \rho^{1/2}$ and $\Phi = \left(\frac{\pi}{2} + \theta\right)\frac{1}{2}$

In the w-plane the unit circle of disturbance becomes a semicircle of radius 1; the back side of the wall lies along the line $\Phi = 0$ while the front side falls along $\Phi = \pi$. The line $\theta = 0$ in the ζ-plane rotates to $\Phi = \frac{\pi}{4}$ and the line $\theta = \pi$ is found along $\Phi = \frac{3\pi}{4}$. Thus in the w-plane the boundary conditions on the semicircle $R = 1$ become

$$\left.\begin{array}{ll} p = 0 & 0 \le \Phi \le \frac{\pi}{4} \\ p = 1 & \frac{\pi}{4} \le \Phi \le \frac{3\pi}{4} \\ p = 2 & \frac{3\pi}{4} \le \Phi \le \pi \end{array}\right\} \qquad (79)$$

Any analytic function of w will also be an analytic function of ζ.

The function $w - e^{i\frac{\pi}{4}}$ is represented by the line BA in Figure E-17 and its argument by the angle α. When A falls on the unit circle, α increases discontinuously from $-\frac{\pi}{4}$ to $\frac{3\pi}{4}$ as A moves counter clockwise through the point B. The function $w - e^{i\frac{5\pi}{4}}$ is continuous within and on the upper semicircle DBE. Furthermore the included angle γ is

$$\gamma = \alpha + \beta$$

where $\text{Arg}\left[w - e^{i\frac{\pi}{4}}\right] = -\alpha$ and $\text{Arg}\left[w - e^{i\frac{5\pi}{4}}\right] = \beta$. But along the arc EB, $\gamma = \frac{\pi}{2}$. Hence the function

$$f_1 = \frac{1}{\pi}\left\{\text{Arg}\left[\frac{w - e^{i\frac{5\pi}{4}}}{w - e^{i\frac{\pi}{4}}}\right] - \frac{\pi}{2}\right\}$$

is zero along EB and 1 along BD.

By a similar argument based on Figure E-18 it is clear that the function

$$f_2 = \frac{1}{\pi}\left\{\text{Arg}\left[\frac{w - e^{i\frac{7\pi}{4}}}{w - e^{i\frac{3\pi}{4}}}\right] - \frac{\pi}{2}\right\}$$

is zero along the arc EB′ and 1 along B′D.

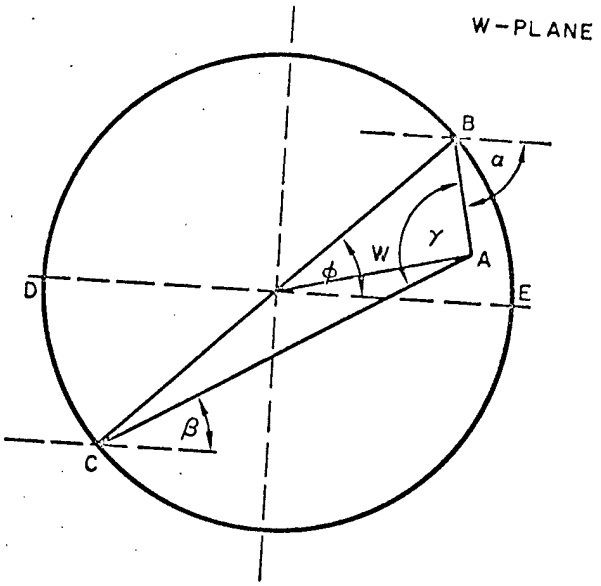

FIGURE E-17 COMPUTATION OF ARGUMENT $\left[\frac{w - e^{5\pi i/4}}{w - e^{\pi i/4}}\right]$

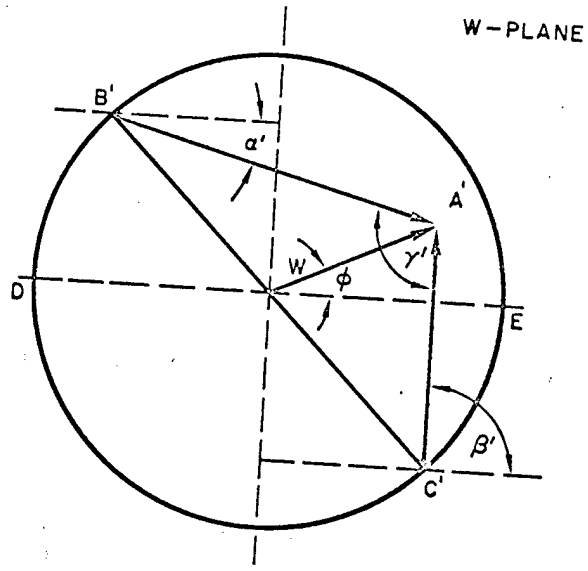

FIGURE E-18 COMPUTATION OF ARGUMENT $\left[\frac{w - e^{7\pi i/4}}{w - e^{3\pi i/4}}\right]$

Thus the sum

$$f_1 + f_2 = \frac{1}{\pi}\left\{ \text{Arg}\left[\frac{w - e^{i\frac{5\pi}{4}}}{w - e^{i\frac{\pi}{4}}} \cdot \frac{w - e^{i\frac{7\pi}{4}}}{w - e^{i\frac{3\pi}{4}}} \right] - \pi \right\} \qquad (80)$$

meets the required boundary conditions along the semicircle EBD in the w-plane. But

$$F(w) = \frac{1}{\pi}\left\{ \ln\left[\frac{w - e^{i\frac{5\pi}{4}}}{w - e^{i\frac{\pi}{4}}} \cdot \frac{w - e^{i\frac{7\pi}{4}}}{w - e^{i\frac{3\pi}{4}}} \right] - i\pi \right\}$$

is analytic in w and z and since $f_1 + f_2$ in Eq. (80) is evidently the imaginary part of F(w), Eq. (80) provides the sought-for expression giving the pressure distribution within and on the circle of disturbance $\rho = R = 1$.

Eq. (80) can be written as

$$\pi p = \tan^{-1}\left(\frac{R \sin \bar{\Phi} + \frac{1}{\sqrt{2}}}{R \cos \bar{\Phi} - \frac{1}{\sqrt{2}}} \right) + \tan^{-1}\left(\frac{R \sin \bar{\Phi} + \frac{1}{\sqrt{2}}}{R \cos \bar{\Phi} - \frac{1}{\sqrt{2}}} \right)$$

$$- \tan^{-1}\left(\frac{R \sin \bar{\Phi} - \frac{1}{\sqrt{2}}}{R \cos \bar{\Phi} - \frac{1}{\sqrt{2}}} \right) - \tan^{-1}\left(\frac{R \sin \bar{\Phi} - \frac{1}{\sqrt{2}}}{R \cos \bar{\Phi} + \frac{1}{\sqrt{2}}} \right) - \pi \qquad (81)$$

where

$$R = \rho^{1/2} = \left[\frac{r}{1 + (1 - r^2)^{1/2}} \right]^{1/2}$$

and

$$\bar{\Phi} = \frac{\pi}{4} + \frac{\theta}{2}$$

The denominators of the four arctangents in (81) have real roots in the range $0 \le \bar{\Phi} \le \pi$ when $\rho \ge 1/2$; and care must be taken to evaluate the inverse functions in such a way that p is continuous within the unit circle. There are no zeros in the denominators when $\rho < \frac{1}{2}$.

If $R \cos \bar{\Phi}_1 + \frac{1}{\sqrt{2}} = 0$ and

$$R \cos \bar{\Phi}_2 - \frac{1}{\sqrt{2}} = 0$$

then $\frac{3\pi}{4} \leq \bar{\Phi}_1 \leq \pi$

and $0 \leq \bar{\Phi}_2 \leq \frac{\pi}{4}$

If the FORTRAN algorithm is used to evaluate the arctangent terms in (81) then for

$$\bar{\Phi} > \bar{\Phi}_2 \text{ and } R > \frac{1}{\sqrt{2}}$$

the second term,

$$\tan^{-1}\left(\frac{R \sin \bar{\Phi} + \frac{1}{\sqrt{2}}}{R \cos \bar{\Phi} - \frac{1}{\sqrt{2}}}\right)$$

may be increased by π, and the third term

$$\tan^{-1}\left(\frac{R \sin \bar{\Phi} - \frac{1}{\sqrt{2}}}{R \cos \bar{\Phi} - \frac{1}{\sqrt{2}}}\right)$$

must be decreased by π, or the sum in (81) increased by 2π. When $\bar{\Phi} > \bar{\Phi}_1$ and $R > \frac{1}{\sqrt{2}}$ we must add another 2π to keep the expression for p continuous and insure the existence of its derivatives.

In order to assure continuity with respect to radius the foregoing choices limit the arctangents to certain quadrants where radius R is such that no zeros in the denominators exist, i.e., when $R < \frac{1}{2}$. Thus, since we have chosen to add π to

$$\tan^{-1}\left(\frac{R \sin \bar{\Phi} + \frac{1}{\sqrt{2}}}{R \cos \bar{\Phi} - \frac{1}{\sqrt{2}}}\right)$$

for $\Phi > \Phi_2$ and $R > \frac{1}{2}$, we must, when using the FORTRAN algorithm, add π to the same inverse tangent for all Φ when $R < \frac{1}{2}$ in order to place the angle computed in the second quadrant. Similarly, by subtracting π from

$$\tan^{-1}\left(\frac{R \sin \Phi - \frac{1}{\sqrt{2}}}{R \cos \Phi - \frac{1}{\sqrt{2}}}\right)$$

when $\Phi > \Phi_2$ and $R > \frac{1}{2}$ we are placing the arctangent in the range $-\frac{\pi}{2}$ to $-\pi$; hence the same function, when $R < \frac{1}{2}$, must be computed in the same range by subtracting π from the angle as computed by FORTAN. When $R < \frac{1}{2}$ the denominator

$$R \cos \Phi + \frac{1}{\sqrt{2}}$$

is always positive and when $R < \frac{1}{2}$ the FORTRAN choices of quadrant for the two arctangents containing it are consistent with those for $R > \frac{1}{2}$.

Pressure contours, located as outlined above, are shown in Figure E-19.

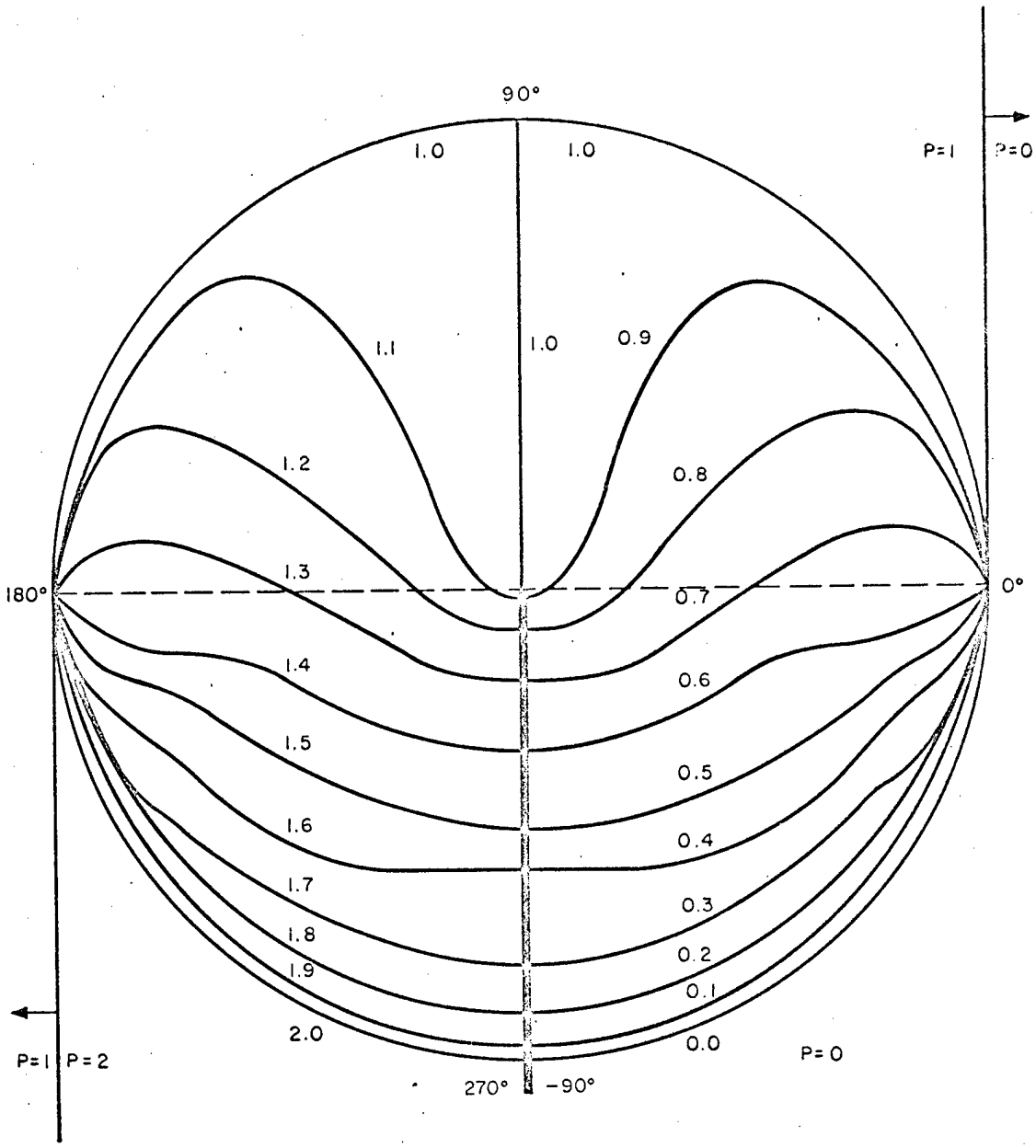

FIGURE E-19 PRESSURE CONTOURS WITHIN CIRCLE OF DISTURBANCE

NOTATION*

A	area of opening or openings through which room fills
$\mathcal{A}$	constant equal to various functions of γ, appearing in Equation (5)
B	constant equal to various functions of γ and/or of interior and exterior conditions, appearing in Equation (5)
c	speed of sound in air
c_v	specific heat at constant volume for air
F	numerical factor for consistency of units
I	integral
K	discharge coefficient
ℓ	distance along jet axis measured from opening
m	mass of air
Δm	increment of air mass corresponding to time increment Δt
P	air pressure
P'	air pressure during immediately preceding time step
P_{lo}	peak overpressure outside front or first wall
P_{lr}	total overpressure outside rear wall
P_c	sum of dynamic and side-on air pressure at time $t = t_c$
P_d	free-field dynamic pressure

* Numerical subscripts may be used with variables to refer to a particular space or volume; see Preface.

P_{dc} dynam[illegible]essure i[illegible]ast wave at time $t = t_c$

P_{do} peak d[illegible]ic press[illegible] in blast wave

P_o ambien[illegible] press[illegible]

P_R reflec[illegible]essure[illegible] wall struck [illegible]last wave

P_s free-[illegible] side-o[illegible] pressure

P_{sc} free[illegible] side-[illegible] verpressur[illegible] $t = t_c$

P_{so} free-[illegible] peak s[illegible] verpressure

p acoust[illegible] ver) pr[illegible]

q dynamic[illegible]sure [illegible]

$\bar{q}$ (spati[illegible] verage [illegible]c pressu[illegible]t at one cross section

R gas co[illegible]t for [illegible]e Ref. 5.)

R radius[illegible]t of s[illegible]ng air

r radial [illegible]dinate, $r = \eta^2 + [illegible]$

r radial [illegible]dinate [illegible]ed from axis [illegible]

S specifi[illegible]tropy [illegible]

ΔS increm[illegible]f entr[illegible]

s wall d[illegible]sion us[illegible]ompute clearin[illegible]

T absolu[illegible]emperatu[illegible]

ΔT filli[illegible]me or int[illegible] between firs[illegible]al of blast and achie[illegible]t of pres[illegible] quilibrium

t time [illegible]ured from [illegible] arrival of [illegible]t structure

t_c clearing time of structure in blast wave

t_o duration of positive side-on overpressure

Δt increment of time

U blast front speed

u particle speed of air

u^* air particle speed along jet axis

V volume of room or other space to be filled

ΔV increment of air volume

v speed of object in air stream

x Cartesian coordinate

y Cartesian coordinate

y unknown variable in Equation (5)

y_o a specific solution of Equation (5), i.e., $y_o = 0.1912$

w complex variable $Re^{i\Phi}$

Δw energy increment

α angle in complex w-plane

α a certain function of y

α acceleration coefficient of object in air stream

β angle in complex w-plane

γ ratio of specific heat at constant pressure to specific heat at constant volume

γ angle in complex w-plane

Δ correction term applied to momentum balance associated with one control surface

ζ complex variable $\rho e^{i\theta}$

η time independent coordinate, i.e., $\eta = y/ct$

θ angle between inward normal to surface and the positive direction of the x-axis

θ angular coordinate, i.e., $\tan \theta = y/x$

ρ density of air

ρ reduced radial coordinate

ρ' air density during immediately preceding time step

ρ_o ambient air density

σ time independent coordinate, i.e., $\sigma = x/ct$

τ time required to transmit a sound signal over the longest room dimension

φ angle in complex w-plane

REFERENCES

1. Glasstone, S., editor, The Effects of Nuclear Weapons, U.S. Dept. of Defense and Atomic Energy Commission, Feb. 1964 reprint (with changes) of 1962 edition

2. Moulton, J., editor, Nuclear Weapons Blast Phenomena, Defense Atomic Support Agency, Washington D.C., DASA 1200 Vol. I, March 1960

3. The Design of Structures to Resist the Effects of Atomic Weapons, EM 1110-345-413, Massachussetts Institute of Technology for the Office of the Chief of Engineers, United States Army, Washington D.C., 1957

4. Iverson, J., Existing Structures Evaluation, Part II: Window Glass and Applications, Stanford Research Institute for the Office of Civil Defense, Menlo Park, Calif., December 1968

5. Eshbach, O. W., editor, Handbook of Engineering Fundamentals, 2nd edition, John Wiley & Sons, 1952, (See chapter 8 for discussion of entropy and internal energy.)

6. Oswatitsch, K., Gas Dynamics, Academic Press, 1956 (for a discussion of the concept and use of control surfaces in the study of flowing compressible fluids)

7. Eshbach, O. W., op. cit., pg 8-23

8. Eshbach, O. W., op. cit., pg 8-21

9. Coulter, G. A., Air Shock Filling of Model Rooms, Ballistic Research Laboratories Memorandum Report No. 1916, Aberdeen Proving Ground, Md., March 1968, Figure 28, pg 54

10. Open Shelter Feasibility Study (DRAFT), The Vertex Corporation, Kensington, Md., June 1968

11. Melichar, J. F., Air-Blast-Induced Aerodynamic Effects in Blast-Slanted Basement Shelters, URS Corporation for Office of Civil Defense, URS 692-3, OCD Work Unit 1126E, Burlingame, Calif., Jan. 1969

12. Melichar, J. F., The Propagation of Blast Waves into Chambers: Aerodynamic Mechanisms, Terminal Ballistics Laboratory, Ballistic Research Laboratories, Aberdeen Proving Ground, Md., November 1967

13. Shapiro, A., The Dynamics and Thermodynamics of Compressible Fluid Flow, Volume I, The Ronald Press Co., 1953 (art. 4.7 for treating flow into a large reservoir which is steadily being evacuated)

14. Bowen, I. G., et al., A Model Designed to Predict the Motion of Objects Translated By Classical Blast Waves, Lovelace Foundation for Medical Education and Research, Albuquerque, N.M., U.S. Atomic Energy Commission CEX-58.9, June 29, 1961

15. Brode, H. L., Point Source Explosion in Air, RM-1824-AEC, The RAND Corporation, December 3, 1956

16. Ludloff, A. F., "On Aerodynamics of Blasts," Advances in Applied Mechanics, Vol. III, R. V. Mises, T. V. Kármán, editors, Academic Press, 1953

17. Kot, C., IIT Research Institute, Chicago, Ill., personal communication

18. Coulter, G. A., op. cit., Figures 19 and 20, pp 43 and 44

19. Coulter, G. A., op. cit., Fig. 7, pg 27

20. Abramovich, G. N., The Theory of Turbulent Jets, M.I.T. Press, 1963

21. Coulter, G. A., Flow in Model Rooms Caused by Air Shock Waves, Ballistic Research Laboratories Memorandum Report No. 2044, Aberdeen Proving Ground, Md., July 1970

22. Melichar, J. F., Analysis of the Effect of Shelter Openings on Blast Protection, URS Research Company, San Mateo, Calif., for U.S. Office of Civil Defense, September 1970

23. Taylor, W. J., Ballistic Research Laboratories, Aberdeen Proving Ground, Maryland, personal communication, March 1971